

Spectral properties of noisy classical and quantum propagators

This content has been downloaded from IOPscience. Please scroll down to see the full text.

2003 Nonlinearity 16 1685

(<http://iopscience.iop.org/0951-7715/16/5/309>)

View [the table of contents for this issue](#), or go to the [journal homepage](#) for more

Download details:

This content was downloaded by: nonnen

IP Address: 132.167.222.3

This content was downloaded on 24/03/2014 at 20:38

Please note that [terms and conditions apply](#).

Spectral properties of noisy classical and quantum propagators

Stéphane Nonnenmacher

Service de Physique Théorique, CEA/DSM/PhT Unité de recherche associée au CNRS
CEA/Saclay, 91191 Gif-sur-Yvette cédex, France

E-mail: nonnen@spt.saclay.cea.fr

Received 15 January 2003, in final form 6 June 2003

Published 11 July 2003

Online at stacks.iop.org/Non/16/1685

Recommended by T Prosen

Abstract

We study classical and quantum maps on the torus phase space, in the presence of noise. We focus on the spectral properties of the noisy evolution operator, and prove that for any amount of noise, the quantum spectrum converges to the classical one in the semiclassical limit. The small-noise behaviour of the classical spectrum highly depends on the dynamics generated by the map. For a chaotic dynamics, the outer spectrum consists of isolated eigenvalues ('resonances') inside the unit circle, leading to an exponential damping of correlations. In contrast, in the case of a regular map, part of the spectrum accumulates along a one-dimensional 'string' connecting the origin with unity, yielding a diffusive behaviour. We finally study the non-commutativity between the semiclassical and small-noise limits, and illustrate this phenomenon by computing (analytically and numerically) the classical and quantum spectra for some maps.

Mathematics Subject Classification: 81Q50, 37D20, 37J35, 37C30, 81S30, 60J60

1. Introduction

Numerical studies of chaotic dynamical systems inevitably face the problem of rounding errors due to finite computer precision. Indeed, the instability of the dynamics would require infinite precision of the initial position, if one wants to compute the long-time evolution. Besides, any deterministic model describing the evolution of some physical system is intrinsically an approximation, which neglects unknown but presumably small interactions with the 'environment'. A way to take this interaction into account is to introduce some randomness in the deterministic equations, for instance through a term of Langevin type. Such a term induces some diffusion, that is, some coarse-graining or smoothing of the phase space density. If the

deterministic part of the dynamics is unstable, it has the opposite effect of transforming long-wavelength fluctuations of the density into short-wavelength ones, so the interplay between both components (deterministic versus random) of the dynamics is *a priori* not obvious. Rigorous results on the behaviour of noisy chaotic systems have been obtained recently [27, 6, 8]: they show that a usual property of deterministic chaos, namely the exponential mixing, still holds in the presence of noise. Actually, introducing some noise provides a way of computing the exponential decay rate (and the subsequent ‘resonances’) in a controlled fashion [1, 26, 31, 35, 34].

In quantum mechanics, a (small) system is never perfectly isolated either, and is subject to inevitable interaction with the environment, responsible for decoherence effects. The study of decoherence has received a lot of attention recently, due to the (mostly theoretical) interest in quantum computation [17] and precise experiments measuring decoherence. In some simple cases, one can study the dynamics of the full system (small plus environment), and obtain the effective dynamics of the small one [14]. Under suitable assumptions, this effective dynamics results in a memoryless (super)operator acting on the quantum density of the small system.

A possible way to modelize this operator is by quantizing the ‘Langevin term’ used in the classical framework, that is introduce a random noise in the quantum evolution equation (for either continuous or discrete-time dynamics). Averaging over the noise yields, in the continuous-time framework, a non-Hermitian ‘Lindblad operator’ [30], while in the discrete-time case the evolution can be cast into the product of a unitary (deterministic) evolution operator with a ‘quantum coarse-graining’ operator [7], this product being called from now on the ‘coarse-grained evolution operator’. Similar operators have also appeared in the theoretical study of spectral correlations for quantized maps [33], and in models of dissipative quantum maps on the sphere [13].

Several recent studies have been devoted to noisy or coarse-grained quantum maps [26, 31, 7] in the semiclassical limit, emphasizing the respective roles of regular versus chaotic regions in the classical phase space. The aim was either to study the time evolution of an initial density [7], or to compute the spectrum of the classical or quantum coarse-grained evolution operators [26, 31]. A different type of quantum dissipation operator, originating from the theory of super-radiance, was composed with a unitary quantum map on the sphere, and studied in a series of papers by Braun [13]. The author computed a Gutzwiller-like semiclassical trace formula for powers of the full (non-unitary) propagator, and showed their connection with traces of the corresponding classical dissipative propagator.

In this paper, we present some results on the spectrum of coarse-grained propagators, for maps defined on the two-dimensional torus (section 2). For the sake of simplicity, we restrict ourselves to either fully chaotic or fully regular maps. In the limit of vanishing noise, the spectrum of the classical coarse-grained evolution operator behaves differently in these two (extreme) cases: for a chaotic map, the spectrum has a finite gap between unity and the next largest eigenvalue, due to exponential decay of correlations [40, 8], while in the regular case some eigenvalues come arbitrarily close to unity. To illustrate these results, we study in detail some linear systems (either chaotic or integrable), for which the eigenvalues may be computed analytically.

We then turn to the quantum version of these systems (section 4). After recalling the setting of quantum maps on the torus, we define the quantum coarse-graining operator, and then prove that for any classical map and a fixed finite noise, the spectrum of the quantum coarse-grained evolution operator converges to the spectrum of the classical one in the semiclassical limit (theorem 1).

We finally study in section 5 the non-commutativity of the semiclassical versus vanishing-noise limits, using as examples the maps studied in the classical framework (section 5). As

a byproduct, we show that one can obtain the resonances of a classical hyperbolic map from the spectrum of an associated quantum operator (the quantum coarse-grained propagator), provided the coarse-graining is set to decrease slowly enough in the semiclassical limit (we conjecture a sufficient condition for the speed of convergence). In contrast, for an integrable map the same limit yields a spectrum densely filling one-dimensional curves (‘strings’) in the unit disc, one of them containing unity as a limit point.

2. Classical noisy evolution

The classical dynamical systems we will study are defined on a two-dimensional symplectic and Riemannian manifold, the torus $\mathbb{T}^2 = \mathbb{R}^2/\mathbb{Z}^2$. The maps are smooth (C^∞), invertible and leave the symplectic form $dp \wedge dq$ (and therefore the volume element $d^2x = dq dp$) invariant: they are canonical diffeomorphisms of \mathbb{T}^2 . Such a map $x = (q, p) \mapsto Mx$ naturally induces a Perron–Frobenius operator $\mathcal{P} = \mathcal{P}_M$ acting on phase space densities $\rho(x) : [\mathcal{P}\rho](x) = \rho(M^{-1}x)$.

2.1. Spectral properties of the classical propagator

In this section we review the spectral properties of the Perron–Frobenius operator \mathcal{P}_M , depending on the map M and on the functional space on which the operator acts. The results presented are not new, but allow us to fix some notation.

2.1.1. Spectrum on $L^2(\mathbb{T}^2)$. For any canonical diffeomorphism M and any $p \geq 1$, the spectrum of \mathcal{P}_M on the Banach space $L^p(\mathbb{T}^2)$ is a subset of the unit circle and admits $\rho_0(x) \equiv 1$ as invariant density. In particular, \mathcal{P} is unitary on $L^2(\mathbb{T}^2)$ and on its subspace $L^2_0(\mathbb{T}^2)$ of zero-mean densities.

One can relate some dynamical properties of the map M with the (unitary) spectrum of \mathcal{P} on $L^2_0(\mathbb{T}^2)$ [18]. For instance, if the dynamics M leaves invariant a non-constant observable $H(x) \in C^0(\mathbb{T}^2)$ (e.g. if M is the stroboscopic map of the Hamiltonian flow generated by H), then all observables of the type $\rho(x) = f(H(x))$ (with f a smooth function) are invariant as well, so that the eigenvalue 1 of \mathcal{P} is infinitely degenerate. The full spectrum of \mathcal{P} will be explicitly given for some integrable maps in section 3.2.

In contrast, the map M is ergodic iff \mathcal{P} has no invariant density in L^2_0 (i.e. if 1 is a simple eigenvalue in L^2). Stronger chaotic properties may be defined in terms of the correlation function between two densities $f, g \in L^2$:

$$C_{fg}(t) \stackrel{\text{def}}{=} \int_{\mathbb{T}^2} dx f(x)g(M^{-t}x) = (f, \mathcal{P}^t g) \tag{1}$$

(the time parameter t will always take integer values). The map M is said to be mixing iff for any f, g , the correlation function behaves for large times as:

$$C_{fg}(t) \xrightarrow{|t| \rightarrow \infty} \int_{\mathbb{T}^2} dx f(x) \int_{\mathbb{T}^2} dx g(x). \tag{2}$$

A slightly weaker property (weak mixing) is equivalent with the fact that \mathcal{P}_M has no eigenvalue in $L^2_0(\mathbb{T}^2)$.

2.1.2. Exponential mixing. For a certain class of maps (e.g. the Anosov maps defined later), the convergence of mixing is exponentially fast, provided the observables f, g are smooth enough. One speaks of *exponential mixing* with a decay rate $\gamma > 0$ if $|C_{fg}(t) - \int f dx \int g dx| \leq K_{fg}e^{-\gamma|t|}$ for a certain constant K_{fg} .

This behaviour can sometimes be explained through the spectral analysis of the Perron–Frobenius operator \mathcal{P} acting on an *ad hoc* functional space \mathcal{B} , with $\mathcal{B} \not\subset L^2$ (in general \mathcal{B} contains some distributions). One proves that the operator \mathcal{P} on \mathcal{B} is *quasi-compact*: its spectrum consists of finitely many isolated eigenvalues $\{\lambda_i\}$ (called *Ruelle–Pollicott resonances*) situated in an annulus $\{r < \lambda_i < \lambda_0 = 1\}$ for some $r > 0$, plus a possible essential spectrum inside the disc of radius r . In that case, assuming for simplicity that each λ_i is a simple eigenvalue with spectral projector Π_i , the spectral decomposition of \mathcal{P} on \mathcal{B} leads to the following asymptotic expansion for $C_{fg}(t)$ in the limit $t \rightarrow \infty$:

$$C_{fg}(t) = \sum_i \lambda_i^t \langle f, \Pi_i g \rangle + O(r^t). \quad (3)$$

In the above expression, the brackets do not refer to a Hermitian structure, but represent the integrals $\int f(x)[\Pi_i g](x) dx$. The first resonance $\lambda_0 = 1$ corresponds to the unique invariant density ρ_0 , and the decay rate (obviously independent of the observables f, g) is given by $\gamma = -\log |\lambda_1|$, respectively, by $-\log r$ if there is no resonance other than unity.

This type of spectrum was first put in evidence in the case of uniformly hyperbolic maps by using Markov partitions to translate the dynamics on the phase space into a simple symbolic dynamics (namely a subshift of finite type) [40]. It was later extended to more general systems, including non-uniformly hyperbolic ones [4]. In the next sections, we will introduce the Anosov diffeomorphisms on the torus, which often serve as a ‘model’ for deterministic chaos.

2.1.3. Anosov diffeomorphism on the two-dimensional torus. In this section we recall the definition and some properties of an Anosov diffeomorphism M on the torus \mathbb{T}^2 [24]. The Anosov property means that at each point $x \in \mathbb{T}^2$, the tangent space $T_x \mathbb{T}^2$ splits into $T_x \mathbb{T}^2 = E_x^s \oplus E_x^u$, where $E_x^{u/s}$ are the local stable and unstable subspaces. The tangent map $d_x M$ sends $E_x^{u/s}$ to $E_{M(x)}^{u/s}$, and there exist constants $A > 0$, $0 < \lambda_s < 1 < \lambda_u$ (independent on x) s.t.

$$\forall t \in \mathbb{N}, \quad \|(d_x M^t)_{|E_x^s}\| \leq A \lambda_s^t \quad \text{and} \quad \|(d_x M^{-t})_{|E_x^u}\| \leq A \lambda_u^{-t}. \quad (4)$$

These inequalities describe the uniform hyperbolicity of M on \mathbb{T}^2 . The splitting of $T_x \mathbb{T}^2$ into $E_x^{u/s}$ has in general regularity $C^{1+\alpha}$ for some $1 > \alpha > 0$, meaning that it is differentiable and its derivatives are Hölder-continuous with coefficient α .

This uniform hyperbolicity implies that M is ergodic and exponentially mixing with respect to the Lebesgue measure (see next section).

Simple examples of Anosov diffeomorphisms are provided by the linear hyperbolic automorphisms of \mathbb{T}^2 , defined by matrices $A \in SL(2, \mathbb{Z})$ with $|\text{tr} A| > 2$. These maps are sometimes referred to as ‘generalized cat maps’, in reference to Arnold’s ‘cat map’ $A_{\text{Arnold}} = \begin{pmatrix} 2 & 1 \\ 1 & 1 \end{pmatrix}$ [3]. We will study in some detail these linear maps and their quantizations, and obtain a rather explicit description of the associated coarse-grained propagators. One can perturb the linear hyperbolic automorphism A with the stroboscopic map φ_H^1 generated by some Hamiltonian $H(x)$ on the torus: $M \stackrel{\text{def}}{=} \varphi_H^1 \circ A$. If the Hamiltonian H is ‘small enough’, the perturbed map M remains Anosov, and topologically conjugated with the linear map A .

2.1.4. Ruelle resonances for Anosov diffeomorphisms. As announced above, Anosov diffeomorphisms on \mathbb{T}^2 are exponentially mixing, and their correlation functions satisfy expansions of the type (3). Although the original proofs made use of Markov partitions [40], we will rather describe a more recent approach due to Blank *et al* [8], which has the advantage of providing spectral results for the coarse-grained propagator as well.

The strategy of [8] is to define a Banach space \mathcal{B} of densities on \mathbb{T}^2 adapted to the map M : the space \mathcal{B} contains distributions which are smooth along the unstable direction of M but possibly singular (dual of smooth) along the stable direction. In particular, these functions are too singular to be in L^2 , which allows a non-unitary spectrum of \mathcal{P} acting on \mathcal{B} . The space \mathcal{B} is defined in terms of an arbitrary parameter $0 < \beta < 1$, and satisfies the continuous one-to-one embeddings: $C^1(\mathbb{T}^2) \rightarrow \mathcal{B} \rightarrow C^1(\mathbb{T}^2)^*$.

The space \mathcal{B} depends on the map M , and also on the direction of time: the space $\mathcal{B}_{M^{-1}}$ adapted to the map M^{-1} is different from \mathcal{B}_M . Although the map M on the torus is invertible, the dynamics of the operator \mathcal{P} on the space \mathcal{B} is *irreversible*: its spectrum is qualitatively very different from that of \mathcal{P}^{-1} .

The authors indeed show that \mathcal{P} is quasi-compact in \mathcal{B} , with essential spectral radius r_{ess} bounded above by $\sigma = \max(\lambda_u^{-1}, \lambda_s^\beta)$ (see equation (4) for the definition of $\lambda_{u/s}$). For any $1 > r > \sigma$, the spectrum of \mathcal{P} in the ring $R_r \stackrel{\text{def}}{=} \{r \leq |\lambda| \leq 1\}$ consists of isolated eigenvalues, the Ruelle–Pollicott resonances $\{\lambda_i\}$. Therefore, a spectral expansion similar to (3) holds for any pair of observables $f, g \in \mathcal{B}$, which includes in particular observables in $C^1(\mathbb{T}^2)$ (the expansion might be slightly more complicated than (3) due to possible finite degeneracies of the resonances).

A possible strategy to extend the results of [8] to maps and observables of regularity C^k was discussed in the recent preprint [5]. Under stronger smoothness assumptions, namely for real-analytic Anosov maps in two dimensions, Rugh [41] constructed a transfer operator acting on observables real-analytic along the unstable direction, and ‘dual of analytic’ along the stable one; he showed that this operator is compact, which means that the essential spectral radius vanishes in that case.

2.2. Coarse-grained classical propagator

In this section we precisely define the operator representing the effect of ‘noise’ on the deterministic evolution of M . This operator is of diffusion type, it realizes a coarse-graining of the densities.

2.2.1. Classical diffusion operator. We consider a smooth probability density $K(x)$ on \mathbb{R}^2 with compact support. For simplicity, we also assume that $K(x) = K(-x)$. From there, to any $\epsilon > 0$ corresponds a probability density on the torus, defined as

$$K_\epsilon(x) = \frac{1}{\epsilon^2} \sum_{n \in \mathbb{Z}^2} K\left(\frac{x+n}{\epsilon}\right).$$

Due to the compact support of K , we see that for small enough ϵ and any $x \in \mathbb{T}^2$ this sum has at most one non-vanishing term (for x close to the origin). We define the coarse-graining operator D_ϵ on $L^2(\mathbb{T}^2)$ as the following convolution:

$$\forall f \in L^2(\mathbb{T}^2), \quad [D_\epsilon f](y) = \int_{\mathbb{T}^2} dx K_\epsilon(y-x) f(x). \tag{5}$$

D_ϵ is a self-adjoint compact operator on $L^2(\mathbb{T}^2)$, with discrete spectrum accumulating at the origin.

We define the Fourier transform on the plane as

$$\tilde{K}(\xi) = \int_{\mathbb{R}^2} dx K(x) e^{2i\pi \xi \wedge x}$$

with the wedge product given by $\xi \wedge x = \xi_1 p - \xi_2 q$. From the assumptions on the density K , the function $\tilde{K}(\xi)$ is real, even and smooth. It takes its maximum at $\xi = 0$ (where it behaves

as $\tilde{K}(\xi) = 1 - Q(\xi) + O(|\xi|^4)$, with $Q(\cdot)$ a positive definite quadratic form), and decreases fast for $|\xi| \rightarrow \infty$.

The plane waves (or Fourier modes) on \mathbb{T}^2 are accordingly defined as $\rho_k(x) \stackrel{\text{def}}{=} \exp\{2i\pi x \wedge k\}$, for $k \in \mathbb{Z}^2$. They obviously form an orthonormal eigenbasis of the coarse-graining operator:

$$\forall \epsilon > 0, \quad \forall k \in \mathbb{Z}^2, \quad D_\epsilon \rho_k = \tilde{K}(\epsilon k) \rho_k. \quad (6)$$

The fast decrease of the eigenvalues as $|k| \rightarrow \infty$ implies that the operator D_ϵ is not only compact, but also trace-class. It kills the small-wavelength modes, effectively truncating the Fourier decomposition of $\rho(x)$ at a cut-off $|k| \sim \epsilon^{-1}$. For some instances, we will actually replace the smooth function $\tilde{K}(\xi)$ by a sharp cut-off $\Theta(1 - |\xi|)$ (with Θ the Heaviside step function).

2.2.2. Classical coarse-grained propagator. The noisy dynamics associated with the map M is represented by the product of the deterministic evolution \mathcal{P}_M with the diffusion operator:

$$\mathcal{P}_{M,\epsilon} \stackrel{\text{def}}{=} D_\epsilon \circ \mathcal{P}_M. \quad (7)$$

It may be more natural to define the noisy propagator as the more ‘symmetric’ $D_\epsilon \circ \mathcal{P}_M \circ D_\epsilon$, but both definitions lead to the same spectral structure. $\mathcal{P}_{M,\epsilon}$ describes a Markov process defined by the deterministic map M followed by a random jump on a scale ϵ .

We now give some general properties of this operator, independent of the particular map M . Like the regularizing operator D_ϵ , $\mathcal{P}_{M,\epsilon}$ maps distributions into smooth functions, and is *compact* and *trace-class* on any functional space containing $C^\infty(\mathbb{T}^2)$ as a dense subspace, with a *spectrum independent of the space*. Its eigenvalues $\{\lambda_{\mu,\epsilon}\}_{\mu \geq 0}$ are inside the unit disc (only $\lambda_{0,\epsilon} = 1$ is exactly on the unit circle), they are of finite multiplicity and admit the origin as the only accumulation point. The eigenvalue $\lambda_{0,\epsilon}$ is simple, with unique eigenfunction ρ_0 . \mathcal{P}_ϵ maps a real density to a real density, therefore its spectrum is symmetric with respect to the real axis.

In the next section we investigate in more detail the behaviour of these eigenvalues in the limit of small noise, stressing the difference between chaotic versus regular maps.

3. Spectral properties of a classical coarse-grained propagator

We describe more precisely the spectrum of $\mathcal{P}_{M,\epsilon}$, in the limit of small noise, and for different classes of maps M . We start with the most chaotic maps, namely the Anosov diffeomorphisms defined in section 2.1.3, the exponential mixing of which was described in section 2.1.4. In the second part, we will then turn to the opposite case of ‘regular’ maps on \mathbb{T}^2 .

3.1. Anosov diffeomorphism

We use the same notation as in section 2.1.4 for M an Anosov map. It was proven in [8] that the spectrum of $\mathcal{P}_{M,\epsilon}$ outside some neighbourhood of the origin converges to the resonance spectrum of \mathcal{P}_M on the Banach space \mathcal{B} .

More precisely, for M a smooth Anosov canonical diffeomorphism on \mathbb{T}^2 with foliations of Hölder regularity $C^{1+\alpha}$ ($0 < \alpha < 1$), one considers the ‘associated’ Banach space $\mathcal{B} = \mathcal{B}_M$ defined in terms of a coefficient $\beta < \alpha$, such that the essential radius of \mathcal{P} on \mathcal{B} has for upper bound $\sigma = \max(\lambda_u^{-1}, \lambda_s^\beta)$. The authors then construct a ‘weak’ norm $\|\cdot\|_w$ on $\mathcal{L}(\mathcal{B})$, such that $\|\mathcal{P}_\epsilon - \mathcal{P}\|_w \rightarrow 0$ as $\epsilon \rightarrow 0$. As a consequence, for any $1 > r > \sigma$, any λ in the annulus $R_r = \{r \leq |\lambda| \leq 1\}$ and any $\delta > 0$ small enough, the spectral projector $\Pi_{B(\lambda,\delta)}^{(\epsilon)}$ of \mathcal{P}_ϵ (respectively, $\Pi_{B(\lambda,\delta)}$ of \mathcal{P}) in the disc $B(\lambda, \delta) = \{z : |z - \lambda| \leq \delta\}$ satisfies

$\|\Pi_{B(\lambda,\delta)}^{(\epsilon)} - \Pi_{B(\lambda,\delta)}\|_w \xrightarrow{\epsilon \rightarrow 0} 0$. Both projectors therefore have the same rank for ϵ small enough, this rank being zero if the disc contains no resonance λ_i .

This proves that the spectrum of \mathcal{P}_ϵ in the annulus R_r converges (with multiplicity) to the set of resonances $\{\lambda_i\}$ as $\epsilon \rightarrow 0$, and the eigenmodes of \mathcal{P}_ϵ weakly converge to corresponding eigenmodes of \mathcal{P} (since the latter are genuine distributions, the convergence can only hold in a weak sense).

Remarks.

- These results also apply to the ‘symmetric’ coarse-graining $D_\epsilon \circ \mathcal{P} \circ D_\epsilon$.
- It is reasonable to conjecture that these results hold as well if the coarse-graining kernel $K(x)$ is not compactly supported on \mathbb{R}^2 , but decreases sufficiently fast, for instance if one takes the Gaussian $G(x) \stackrel{\text{def}}{=} e^{-\pi|x|^2}$, $\tilde{G}(\xi) = e^{-\pi|\xi|^2}$, as was done in [1, 26]. As a broader generalization, we will sometimes consider a coarse-graining defined by a sharp cut-off in Fourier space, $\tilde{K}(\xi) = \Theta(1 - |\xi|)$, similar to the method used in [31]; a finite-rank coarse-graining was also used in [34] for one-dimensional noisy maps.
- If the map M and the kernel $K(x)$ are real-analytic, we conjecture that the eigenvalues of \mathcal{P}_ϵ on any ring R_r with $r > 0$ converge to the resonances \mathcal{P} in R_r (cf the remark at the end of section 2.1.4).

The (discrete) spectrum of \mathcal{P}_ϵ is the same on any space \mathcal{S} admitting C^∞ as dense subspace, in particular on L^2 , and this is the space we will consider from now on (more precisely, its subspace L^2_0). This spectrum drastically differs from the absolutely continuous unitary spectrum of the ‘pure’ propagator \mathcal{P} on that space (cf section 2.1). The unitary spectrum is thus *unstable* upon the coarse-graining D_ϵ : when switching on the noise, the spectral radius of \mathcal{P}_ϵ on L^2_0 suddenly collapses from 1 to $|\lambda_1| < 1$. As we will see in the next sections, this collapse is characteristic of chaotic maps. We first describe it explicitly for the case of hyperbolic linear automorphisms.

3.1.1. Example of Anosov maps: the hyperbolic linear automorphisms. In this section we review [18, 27] the spectral analysis of the (pure versus noisy) propagator when the map A is a hyperbolic linear automorphism of \mathbb{T}^2 (cf section 2.1.3). The unitary operator \mathcal{P}_A on L^2_0 acts very simply on the basis of Fourier modes $\rho_k, k \in \mathbb{Z}^2_* = \mathbb{Z}^2 \setminus 0$, namely as a permutation:

$$[\mathcal{P}_A \rho_k](x) = \rho_k(A^{-1}x) = \rho_{Ak}(x). \tag{8}$$

This evolution induces *orbits* on the Fourier lattice \mathbb{Z}^2_* , which we will denote by $O(k_0) = \{A^t k_0, t \in \mathbb{Z}\}$. Due to the hyperbolicity of A , each orbit is infinite, so that the modes $\{\rho_{A^t k_0}, t \in \mathbb{Z}\}$ span an infinite-dimensional invariant subspace of L^2_0 , which we call $\text{Span } O(k_0)$. The spectral measure of \mathcal{P}_A associated with this subspace is of Lebesgue type (as usual when the operator acts as a shift [39]). The number of distinct orbits being infinite, the spectrum of \mathcal{P}_A on L^2_0 is Lebesgue with infinite multiplicity.

Now we consider the coarse-grained propagator $\mathcal{P}_{\epsilon,A} = D_\epsilon \circ \mathcal{P}_A$. Since the ρ_k are eigenfunctions of D_ϵ (cf equation (6)), $\mathcal{P}_{\epsilon,A}$ will also act as a permutation inside each orbit $O(k_0)$, but now at each step the mode ρ_k is multiplied by $\tilde{K}(\epsilon k)$. Therefore, the operator $\mathcal{P}_{\epsilon,A}$ restricted to the invariant subspace $\text{Span } O(k_0)$ can be represented as follows (the notation (\cdot, \cdot) denotes the scalar product on L^2_0):

$$\mathcal{P}_{\epsilon,A|O(k_0)} = \sum_{t \in \mathbb{Z}} \tilde{K}(\epsilon A^{t+1} k_0) (\rho_{A^t k_0}, \cdot) \rho_{A^{t+1} k_0}. \tag{9}$$

Since $|A^t k_0| \rightarrow \infty$ for $t \rightarrow \pm\infty$, the factors $\tilde{K}(\epsilon A^{t+1} k_0)$ vanish in both limits. As a result, the spectrum of $\mathcal{P}_{\epsilon,A|O(k_0)}$ reduces to the single point $\{0\}$ (which is *not* an eigenvalue, but essential

spectrum) [39]. By taking all orbits into account, the spectrum of $\mathcal{P}_{\epsilon,A}$ on L_0^2 also reduces to $\{0\}$: for linear hyperbolic maps, the collapse of the Lebesgue unitary spectrum through coarse-graining is ‘maximal’.

3.2. Coarse-graining of regular dynamics

In the previous sections we have considered classical propagators of Anosov diffeomorphisms on \mathbb{T}^2 . We now describe the opposite case of an *integrable* map on \mathbb{T}^2 . The notion of integrability for a map is not so clear as for a Hamiltonian flow. In view of the examples below, the definition should include the stroboscopic map $M_H = \varphi_H^1$ of the flow generated by an autonomous Hamiltonian $H(x)$ on \mathbb{T}^2 , but it should also encompass elliptic and parabolic automorphisms, as well as rational translations. A required property is that the phase space \mathbb{T}^2 splits into a union of invariant one-dimensional (not necessarily connected) closed submanifolds, with possible ‘critical energies’. Note that this condition excludes the (un)stable manifolds of an Anosov map, which are open. A more or less equivalent condition for integrability is that the map leaves invariant a nowhere constant smooth function $H(x)$, the level curves of which provide the above submanifolds. As a result, any density $\rho(x) = f(H(x))$ is invariant through \mathcal{P}_M as well, so that \mathcal{P}_M has an infinite-dimensional eigenspace of invariant densities on L_0^2 (which we will call V_{inv}).

The rest of the spectrum of \mathcal{P}_M can be of various types, as we will see (it can be pure point or absolutely continuous, be a mixture, etc). For this reason, a general statement concerning the coarse-grained spectrum of these maps cannot be very precise.

In the following sections we consider some simple examples of integrable maps for which (part of) the spectrum can be analysed in detail. We then discuss (mostly by hand-waving) the general case.

3.2.1. Translations on the torus. The simplest nontrivial maps on \mathbb{T}^2 are the translations $x \mapsto T_v x = x + v \pmod{\mathbb{T}^2}$, which do not derive from a Hamiltonian on the torus. A translation is either ergodic (yet non-mixing) or integrable (see later).

The spectrum of the corresponding Perron–Frobenius operator $\mathcal{P}_v = \mathcal{P}_{T_v}$ on L_0^2 is easy to describe [18]: \mathcal{P}_v admits the Fourier modes ρ_k as eigenstates, with eigenvalues $e^{2i\pi k \wedge v}$. The spectrum of \mathcal{P}_v is therefore pure point, with possible degeneracies. The spectrum of the coarse-grained propagator $\mathcal{P}_{\epsilon,v} = D_\epsilon \circ \mathcal{P}_v$ on L_0^2 is also easy to describe: each Fourier mode ρ_k is an eigenfunction with eigenvalue $\tilde{K}(\epsilon k) e^{2i\pi k \wedge v}$ inside the unit disc. From the small- ϵ expansion $\tilde{K}(\epsilon k) \sim 1 - \epsilon^2 Q(k)$, the eigenvalues corresponding to long wavelengths ($|k| \ll \epsilon^{-1}$) are close to the unit circle for small ϵ , while the short wavelength eigenvalues ($|k| \gg \epsilon^{-1}$) accumulate near the origin. We now describe how the global aspect of the spectrum qualitatively depends on the translation vector v .

- T_v is ergodic iff the coefficients v_1, v_2 as well as their ratio v_1/v_2 are irrational: in that case, the equation $k \wedge v \in \mathbb{Z}$ has no solution for $k \neq 0$. The spectrum of \mathcal{P}_v forms a dense subgroup of the unit circle, all eigenvalues being simple. In the limit $\epsilon \rightarrow 0^+$, the spectrum of $\mathcal{P}_{\epsilon,v}$ becomes ‘dense’ in the unit disc (a similar quantum spectrum is plotted in figure 4, right).
- If one of the coefficients $v_1, v_2, v_1/v_2$ is rational, T_v leaves invariant a family of parallel one-dimensional ‘affine’ submanifolds, and is therefore integrable according to our definition. For instance, if we take $v_1 = r/s$ (with r, s coprime integers) and v_2 irrational, then for any $q_0 \in [0, 1]$, the union of vertical lines $\bigcup_{l=0}^{s-1} \{q = q_0 + l/s\}$ is invariant (if $s > 1$, this set is non-connected). The spectrum of \mathcal{P}_v is still dense on the circle, but all

eigenvalues are now infinitely degenerate: for any k_0 , the modes $k = k_0 + (0, js)$, $j \in \mathbb{Z}$ share the eigenvalue $e^{2i\pi k_0 \wedge v}$. The eigenvalues of $\mathcal{P}_{\epsilon, v}$ are at most finitely degenerate: to each phase $e^{2i\pi k_0 \wedge v}$ corresponds a ‘string’ of eigenvalues of decreasing moduli, the largest one being at a distance $\sim \epsilon^2$ from the unit circle. As in the previous case, the spectrum densely fills the unit disc as $\epsilon \rightarrow 0$.

- If both v_1, v_2 are rational of the form $r_1/s, r_2/s$ with $\text{gcd}(r_1, r_2, s) = 1$, each point of \mathbb{T}^2 is periodic with period s , the map is integrable. The only eigenvalues of \mathcal{P}_v are of the phases $e^{2i\pi j/s}$, all being infinitely degenerate. The eigenvalues of $\mathcal{P}_{\epsilon, v}$ are at most finitely degenerate, they are grouped into s strings of phases $e^{2i\pi j/s}$, $j = 0, \dots, s - 1$. For small ϵ , the eigenvalues become dense along these strings, the largest eigenvalue at a distance $\sim \epsilon^2$ from the unit circle (this spectrum is similar to the quantum one plotted in figure 4, left).

Comparing the first and second cases, we see that the spectrum of \mathcal{P}_ϵ cannot unambiguously differentiate an ergodic from an integrable map: both may have eigenvalues close to the unit circle. On the other hand, the second and third cases both correspond to integrable maps. Yet, their small-noise spectra look quite different from one another.

3.2.2. Non-hyperbolic linear automorphisms of the torus. Another class of non-mixing linear maps on \mathbb{T}^2 is provided by the non-hyperbolic linear automorphisms. These automorphisms split into two classes (for notation, we refer to section 3.1.1):

- The elliptic transformations ($|\text{tr}A| < 2$), such as for instance the $\pi/2$ -rotation given by the matrix $J = \begin{pmatrix} 0 & -1 \\ 1 & 0 \end{pmatrix}$. As opposed to the hyperbolic case, each Fourier orbit $O(k_0) = \{J^j k_0, j = 0, \dots, 3\}$ is finite of period 4, and $\text{Span } O(k_0)$ splits into four eigenspaces associated with the eigenvalues $\{i^l, l = 0, \dots, 3\}$. Switching on coarse-graining, the eigenvalues of $\mathcal{P}_{\epsilon, J}$ read $i^l \lambda_{k_0}$, with $\lambda_{k_0} = \sqrt{|\tilde{K}(\epsilon k_0) \tilde{K}(\epsilon J k_0)|}$. The spectrum of $\mathcal{P}_{\epsilon, J}$ on L_0^2 therefore consist of four strings along the four half-axes, which become dense in the limit $\epsilon \rightarrow 0$ (see figure 1 for the analogous quantum spectrum). Similarly, an elliptic transformation of trace $\text{tr}A = 1$ will satisfy $A^6 = 1$, therefore the spectrum of $\mathcal{P}_{\epsilon, A}$ forms six strings. An elliptic transformation of trace $\text{tr}A = -1$ will lead to three strings.
- The parabolic transformations (or parabolic shears), given by matrices of the type $S = \begin{pmatrix} 1 & s \\ 0 & 1 \end{pmatrix}$, $s \in \mathbb{Z}_*$. The dynamics reads $(q, p) \mapsto (q + sp, p)$, so any periodic function of the momentum p is a conserved quantity. The Fourier vector $k_0 = (k_1, k_2)$ generates the orbit $O(k_0) = \{k_0 + (jsk_2, 0), j \in \mathbb{Z}\}$: if $k_2 = 0$, the mode ρ_{k_0} is invariant and the orbit is a singleton; in contrast, if $k_2 \neq 0$, $O(k_0)$ is infinite, and leads to the Lebesgue spectrum for $\mathcal{P}_{S|O(k_0)}$. The full spectrum of \mathcal{P}_S on L_0^2 is therefore the union of the infinitely degenerate eigenvalue 1 with a countable Lebesgue spectrum [18]. In the case $k_2 \neq 0$, the noisy propagator $\mathcal{P}_{\epsilon, S}$ acts on $\text{Span } O(k_0)$ as in equation (9), upon replacing A by S . Since the wavevectors $|S^t k_0|$ diverge in both limits $t \rightarrow \pm\infty$, the associated spectrum reduces to the singleton $\{0\}$. In contrast, each mode $\rho_{(l, 0)}$ is an eigenstate of $\mathcal{P}_{\epsilon, S}$ with eigenvalue $\tilde{K}(\epsilon(l, 0))$: these modes form a string along the real axis, which becomes dense as $\epsilon \rightarrow 0$.

3.2.3. Nonlinear shear. If we perturb the linear parabolic shear S (cf last section) with the stroboscopic map of the flow generated by a Hamiltonian of the form $F(p)$, we obtain a nonlinear shear $(q, p) \mapsto (q + sp + F'(p), p)$. We assume that $s > 0$, and that the Hamiltonian F satisfies $s + F''(p) > 0$ everywhere. This map still conserves momentum, so that any density $\rho(p)$ is invariant. Among these, the Fourier modes $\rho_{(l, 0)}$ are eigenstates of \mathcal{P}_ϵ , with eigenvalues $\tilde{K}(\epsilon(l, 0))$: they form the same string of real eigenvalues as for the linear shear.

For any $n \in \mathbb{Z}_*$, \mathcal{P} and \mathcal{P}_ϵ leave invariant the subspace $V_n = \text{Span}\{e^{2i\pi nq} \rho(p), \rho \in L^2(\mathbb{T}^1)\}$, and their spectra on this subspace can be partially described, at least if one takes F' small enough and replaces the kernel $\tilde{K}(\xi)$ by the sharp cut-off $\Theta(1 - |\xi_1|)\Theta(1 - |\xi_2|)$ (such that D_ϵ projects to a finite-dimensional subspace). The spectrum of \mathcal{P} on V_n is absolutely continuous, while that of \mathcal{P}_ϵ is contained in a small neighbourhood of the origin, uniformly with respect to n and ϵ (see appendix A.1 for details). The spectrum should be qualitatively the same if $\tilde{K}(\xi)$ is of fast decrease at infinity.

3.2.4. Stroboscopic map of the Harper Hamiltonian flow. As a last example of an integrable map, we consider the Harper Hamiltonian on the torus

$$H(x) = \cos(q) + \cos(p) = \frac{1}{2}(\rho_{(1,0)} + \rho_{(-1,0)} + \rho_{(0,1)} + \rho_{(0,-1)})$$

and take its stroboscopic map $M = \varphi_H^1$. The invariant densities are of the form $\rho(x) = f(H(x))$. As opposed to what happened for the parabolic shear, V_{inv} is not invariant through the diffusion operator D_ϵ , so the spectrum of \mathcal{P}_ϵ is more complicated to analyse. Still, if we take a coarse-graining kernel satisfying $\tilde{K}(\xi) = \tilde{k}(|\xi_1| + |\xi_2|)$ along the axes of slopes $0, \pm\frac{1}{2}, \pm 1, \pm 2, \infty$ then the invariant functions $H(x)$, $(H(x))^2 - 1$ and $(H(x))^3 - \frac{9}{4}H(x)$ are eigenstates of D_ϵ and therefore of \mathcal{P}_ϵ , with respective eigenvalues $\tilde{k}(\epsilon)$, $\tilde{k}(2\epsilon)$ and $\tilde{k}(3\epsilon)$ (if the kernel only satisfies $\tilde{K}((0, \zeta)) = \tilde{K}((\zeta, 0))$ together with even parity, then $H(x)$ will be an eigenstate of \mathcal{P}_ϵ with eigenvalue $\tilde{K}((\epsilon, 0))$). These eigenvalues are real and approach unity as $\epsilon \rightarrow 0$. Numerically, they are the first three elements (respectively, the first element) of a string of real eigenvalues connecting unity to the origin, the further elements of the string being mixtures of invariant and non-invariant densities (see figure 5, right, for a similar quantum spectrum).

3.2.5. General behaviour for an integrable map. After these examples, we want to describe the spectrum of $\mathcal{P}_{M,\epsilon}$ for M an integrable map, say the stroboscopic map of an autonomous Hamiltonian H . As we already explained, the space V_{inv} of invariant densities is infinite-dimensional, containing all densities $f(H(x))$. When applying the coarse-graining D_ϵ , one generally mixes these invariant densities with non-invariant ones (as opposed to what happens for the linear maps described above). Using ideas of degenerate perturbation theory, we conjecture the following behaviour, which is supported by numerical investigations [31, 26].

The invariant subspace V_{inv} contains modes ρ_{lw} with long-wavelength fluctuations (i.e. densities for which the Fourier spectrum is concentrated in a finite region near $k = 0$). For ϵ small, these modes are hardly modified by the coarse-graining operator: $D_\epsilon \rho_{\text{lw}} - \rho_{\text{lw}} = O(\epsilon^2)$. This suggests that \mathcal{P}_ϵ has an eigenstate of the type $\rho_{\text{lw}} + O(\epsilon^2)$, of eigenvalue $1 - O(\epsilon^2)$, this eigenstate being close to an invariant state of \mathcal{P} . In contrast, V_{inv} also contains highly fluctuating modes, which will be very damped by D_ϵ , and should lead to eigenstates of \mathcal{P}_ϵ close to the origin. As a whole, the hybridization of invariant modes with non-invariant ones leads to a string of eigenvalues connecting unity to the origin, this string being symmetrical with respect to the real axis. Note that the projected operator $\Pi_{\text{inv}} \mathcal{P}_\epsilon \Pi_{\text{inv}} = \Pi_{\text{inv}} D_\epsilon \Pi_{\text{inv}}$ (where Π_{inv} is the orthogonal projector on the space V_{inv}) is self-adjoint, therefore its spectrum can be estimated through the min–max method: for $\epsilon \rightarrow 0$ it consists in a dense string of eigenvalues between unity and zero. I believe that the largest eigenstates (-values) of this projected operator are close to eigenstates (-values) of \mathcal{P}_ϵ .

Conclusion: qualitatively different spectra. We have exhibited a qualitative difference of the coarse-grained Perron–Frobenius spectra between, on the one hand, the chaotic maps (Anosov), and on the other hand, non-mixing maps, including ergodic translations and integrable maps.

In the latter case, the spectrum of \mathcal{P}_ϵ on the subspace $L^2_0(\mathbb{T}^2)$ comes close to the unit circle for small ϵ , either along one-dimensional strings ‘connecting’ the origin to infinitely degenerate eigenvalues of \mathcal{P} (among which unity), or by densely filling the unit disc (for ergodic translations). A common feature is that any annulus $\{R < |\lambda| < 1\}$ (or any open neighbourhood of unity) contains more and more eigenvalues of \mathcal{P}_ϵ in the small-noise limit $\epsilon \rightarrow 0$.

In contrast, for an Anosov map the spectrum of \mathcal{P}_ϵ on L^2_0 is contained inside a disc of radius $R < 1$, uniformly for small enough ϵ . This spectrum consists in a finite number (possibly zero) of finitely degenerate eigenvalues (asymptotically close to the Ruelle resonances) inside an annulus $\{r < |\lambda_{\mu,\epsilon}| \leq R\}$, the remaining eigenvalues having moduli smaller than r .

The numerical results of [31, 26] go beyond this statement: the authors consider systems with mixed dynamics (not to be mistaken with the ‘mixing’ property of Anosov maps), that is systems for which the phase space splits into ‘regular islands’ embedded in a ‘chaotic sea’. They study the spectrum of the coarse-grained Perron–Frobenius operator (the coarse-graining is taken as a cut-off in Fourier space), and show the presence of eigenvalues close to the unit circle, the eigendensities of which are supported on the regular islands; on the other hand, they also find some eigenvalues inside the unit circle, which are associated with the chaotic part of phase space, and therefore interpreted as (generalized) Ruelle resonances. Yet, the nature of the ‘chaotic sea’ in such systems is not well understood at the mathematical level, so that a rigorous spectral analysis of the propagator seems a quite distant goal.

4. Quantum coarse-grained evolution

After studying the effect of noise on classical propagators, we turn to noisy quantum maps, obtained by quantizing the classical ones. Although we will restrict ourselves to maps on the 2-torus, the main result of this section (theorem 1) can be straightforwardly generalized to quantum maps on any compact phase space, provided one adapts the definition of the coarse-graining operator (see the discussion in section 4.2.3). We start by recalling the setting of quantized maps on the 2-torus.

4.1. Quantum propagator on the torus

4.1.1. Quantum Hilbert space and observables. We briefly review the construction of quantum mechanics on \mathbb{T}^2 , in order to fix notation. For any value of $\hbar > 0$, the Weyl–Heisenberg group associates with each vector $v = (v_1, v_2) \in \mathbb{R}^2$ the ‘quantum translation’ $\hat{T}_v = \exp\{(i/\hbar)(v_2\hat{q} - v_1\hat{p})\}$ which acts unitarily on $L^2(\mathbb{R})$. These translations satisfy the group relations $\hat{T}_v\hat{T}_{v'} = e^{-(i/2\hbar)v \wedge v'}\hat{T}_{v+v'}$.

The ‘torus wavefunctions’ are then defined as distributions $|\psi\rangle \in \mathcal{S}'(\mathbb{R})$ satisfying the periodicity conditions $\hat{T}_{(0,1)}|\psi\rangle = \hat{T}_{(1,0)}|\psi\rangle = |\psi\rangle$. Due to the group relations, such distributions exist iff \hbar satisfies the condition $(2\pi\hbar)^{-1} = N \in \mathbb{N}$ (such a value of \hbar will be called admissible). In that case they form a space of dimension N , which will be denoted \mathcal{H}_N [23]. A basis of this space is provided by the ‘Dirac combs’ $\{|q_j\rangle_N\}_{j=0,\dots,N-1}$ defined as:

$$\langle q|q_j\rangle_N = \sum_{v \in \mathbb{Z}} \delta(q - q_j - v), \quad \text{with } q_j = \frac{j}{N}. \tag{10}$$

By construction, $|q_j\rangle_N = |q_{j+N}\rangle_N$, so the index j must be understood modulo N . For practical reasons, we will choose the following representatives of integers modulo N : $\mathbb{Z}_N = \{-N/2 + 1, \dots, N/2\}$ for N even, $\mathbb{Z}_N = \{-(N-1)/2 + 1, \dots, (N-1)/2\}$ for N odd.

The quantum translation \hat{T}_v acts inside \mathcal{H}_N iff v is on the square lattice of side $1/N$, that is $v = (V_1/N, V_2/N)$ with $V_i \in \mathbb{Z}$. Besides, each translation with integer coefficients acts on \mathcal{H}_N as a multiple of the identity. As a result, the set $\{\hat{T}_{V/N}, V \in \mathbb{Z}_N^2\}$ forms a basis of the space of linear operators on \mathcal{H}_N , denoted by $\mathcal{L}(\mathcal{H}_N)$. This basis can be used to define the Weyl quantization of smooth observables $f \in C^\infty(\mathbb{T}^2)$. From the Fourier decomposition $f = \sum_{k \in \mathbb{Z}^2} \tilde{f}(k) \rho_k$, the Weyl quantization of the observable f is defined as

$$\hat{f} = Op_N(f) \stackrel{\text{def}}{=} \sum_{k \in \mathbb{Z}^2} \tilde{f}(k) \hat{T}_{k/N} = \sum_{k \in \mathbb{Z}_N^2} \hat{T}_{k/N} \left(\sum_{v \in \mathbb{Z}^2} (-1)^{Nv_1v_2+k \wedge v} \tilde{f}(k + Nv) \right). \tag{11}$$

The ‘converse’ of Weyl quantization, that is the *Weyl symbol* (or Wigner function) $W_{\hat{B}}(x)$ of an operator $\hat{B} \in \mathcal{L}(\mathcal{H}_N)$ is also easily defined through its Fourier transform: for each $k \in \mathbb{Z}^2$, its Fourier coefficient $\tilde{W}_{\hat{B}}(k)$ is given by $\tilde{W}_{\hat{B}}(k) = (1/N) \text{tr}(\hat{T}_{k/N}^\dagger \hat{B})$. These Fourier coefficients are N -periodic (up to a sign), so that the ‘function’ $W_{\hat{B}}(x)$ is a periodic combination of Dirac peaks on the lattice of side $1/2N$ [23]. Alternatively, a *polynomial Weyl symbol* was defined in [19] as the finite sum

$$W_{\hat{B}}^P(x) = \sum_{k \in \mathbb{Z}_N^2} \tilde{W}_{\hat{B}}(k) e^{2i\pi x \wedge k}.$$

As opposed to the former symbol, the polynomial symbol depends on the specific choice for the representative \mathbb{Z}_N (the choice we made, with maximum symmetry around the origin, seems more natural in this respect). The polynomial symbol map together with Op_N yield an *isometric isomorphism* between the subspace $\mathcal{I}_N \stackrel{\text{def}}{=} \text{Span}\{\rho_k, k \in \mathbb{Z}_N^2\}$ of $L^2(\mathbb{T}^2)$ and the space of observables on \mathcal{H}_N equipped with the Hilbert–Schmidt scalar product $(\hat{B}, \hat{C}) = (1/N) \text{tr}(\hat{B}^\dagger \hat{C})$. Since the Hilbert–Schmidt norm differs from the usual operator norm on $\mathcal{L}(\mathcal{H}_N)$, we will denote by L_N^2 the space of observables on \mathcal{H}_N (i.e. $N \times N$ matrices) equipped with the Hilbert–Schmidt norm.

4.1.2. Quantization of canonical maps. We briefly explain how one quantizes a canonical map M on \mathbb{T}^2 . The aim is to define for each $N \in \mathbb{N}$ a unitary operator on \mathcal{H}_N (which we will denote by \hat{M}_N or simply \hat{M}) which satisfies prescribed semiclassical properties [42]. These properties do not unambiguously define the sequence of unitary matrices, so a choice has to be made (in [44], a Toeplitz quantization is proposed for symplectic maps on Kähler manifolds). We present here another quantization prescription, which uses the following decomposition of any canonical map M on \mathbb{T}^2 [16]:

$$M = A \circ T_v \circ \varphi_H^1. \tag{12}$$

In this formula, the linear automorphism $A \in SL(2, \mathbb{Z})$ and the translation T_v are uniquely defined. In contrast, the last factor corresponds to the stroboscopic map of the flow of a time-dependent periodic Hamiltonian $H \in C^\infty(\mathbb{T}_x^2 \times \mathbb{T}_t)$; this Hamiltonian is not unique, since two Hamiltonians $H_1 \neq H_2$ may lead to the same stroboscopic map $\varphi_{H_1}^1 = \varphi_{H_2}^1$. From this decomposition, one can quantize M as follows [25]. First, one quantizes *à la* Weyl the Hamiltonian $H(x, t)$ into the operator $\hat{H}(t)$ on \mathcal{H}_N , then take for the quantization of φ_H^1 the time-ordered exponential $\mathcal{T}e^{-i \int_0^1 dt \hat{H}(t)/\hbar}$. Second, one may quantize the translation T_v with the quantum translation $\hat{T}_{v^{(N)}}$, where the vector $v^{(N)}$ belongs to the $1/N$ -lattice and is close to v , for instance take

$$v^{(N)} = \frac{([Nv_1], [Nv_2])}{N}$$

[32]. Third, provided A satisfies the condition $A \equiv \text{Id}_2 \pmod{2}$ or $A \equiv \sigma_x \pmod{2}$, the linear automorphism A is ‘naturally’ quantized into a unitary matrix \hat{A}_N [23] (this condition may

be relaxed if one generalizes the quantum Hilbert space \mathcal{H}_N to arbitrary ‘Bloch angles’ [12]). Finally, the map M is quantized on \mathcal{H}_N as the product:

$$\hat{M}_N = \hat{A}_N \circ \hat{T}_{v^{(N)}} \circ \mathcal{T} e^{-i2\pi N \int_0^1 dt \hat{H}(t)}. \tag{13}$$

This choice for the quantum map automatically satisfies the Egorov property [12, 32]: for any classical observable $\rho \in C^\infty(\mathbb{T}^2)$,

$$\hat{M}_N \mathcal{O} p_N(\rho) \hat{M}_N^{-1} - \mathcal{O} p_N(\rho \circ M^{-1}) \xrightarrow{N \rightarrow \infty} 0. \tag{14}$$

This means that the quantization and finite-time evolution of densities commute in the semiclassical limit (the convergence holds for the operator norm in $\mathcal{L}(\mathcal{H}_N)$).

In practice, the classical maps we consider are all defined as products of automorphisms, translations and Hamiltonian maps, so they admit a ‘natural’ quantization.

4.1.3. Propagator of quantum densities. The quantum map \hat{M} propagates quantum states $|\psi\rangle \in \mathcal{H}_N$. A density matrix $\hat{\rho}$ is an element of the space $L_N^2 = \mathcal{H}_N \otimes \mathcal{H}_N^*$, and its evolution through the quantum map reads $\hat{\rho} \mapsto \hat{M}\hat{\rho}\hat{M}^{-1} = \text{ad}(\hat{M})\hat{\rho}$. The operator $\hat{\mathcal{P}}_M \stackrel{\text{def}}{=} \text{ad}(\hat{M})$ acting on the space L_N^2 is the quantum analogue of the Perron–Frobenius operator \mathcal{P}_M acting on classical densities. $\hat{\mathcal{P}}_M$ is unitary, with eigenvalues $\{e^{i(\theta_j - \theta_i)}; i, j = 1, \dots, N\}$, where $\{e^{i\theta_j}\}$ are the eigenvalues of the matrix \hat{M} . In contrast with its classical analogue, the space of invariant densities through $\hat{\mathcal{P}}_M$ is at least N -dimensional, since it contains all the rank-1 projectors $|\phi_i\rangle\langle\phi_i|$, where $|\phi_i\rangle$ are the eigenstates of \hat{M} .

The operator $\hat{\mathcal{P}}$ acting on densities is called a *super-operator*, to contrast with an operator acting on \mathcal{H}_N . Being the adjoint action of a unitary matrix, it conserves the *purity* of the density, which means that a pure density $\hat{\rho} = |\psi\rangle\langle\psi|$ is mapped onto a pure density $\hat{\mathcal{P}}\hat{\rho} = |\psi'\rangle\langle\psi'|$. We notice that $\hat{\mathcal{P}}$ conserves the trace of the density, that is the quantum counterpart of the total probability of the density ρ .

4.2. Quantum coarse-graining operator

As we remarked above, the spectrum of $\hat{\mathcal{P}}$ on L_N^2 is qualitatively different from that of \mathcal{P} on $L^2(\mathbb{T}^2)$: the former has at least N invariant eigenstates, while the latter may have only one if the map M is ergodic. In section 2.1, we explained how the spectrum of \mathcal{P} was sensitive to the functional space on which \mathcal{P} acts. This is no longer the case in the quantum framework, since the propagator is a finite-dimensional matrix. Still, we showed in section 3 an alternative way to obtain the (non-unitary) resonance spectrum of an Anosov map, namely by introducing some noise and studying the spectrum of the noisy propagator $\mathcal{P}_\epsilon = D_\epsilon \circ \mathcal{P}$ on the space $L^2(\mathbb{T}^2)$. This procedure can also be carried out at the quantum level, by first defining a ‘quantum coarse-graining’ or ‘quantum diffusion’ (super)operator \hat{D}_ϵ , using it to construct a quantum coarse-grained propagator $\hat{\mathcal{P}}_\epsilon$, then studying the spectrum of the latter on L_N^2 . To connect the classical and quantum frameworks, we will consider the semiclassical limit $N \rightarrow \infty$.

4.2.1. Definition. We define the coarse-graining superoperator by analogy with the classical one (equation (5)). The latter can be expressed as follows:

$$\forall f \in L^2(\mathbb{T}^2), \quad (D_\epsilon f)(x) = \int_{\mathbb{T}^2} dv K_\epsilon(v) \rho(x - v) = \int_{\mathbb{T}^2} dv K_\epsilon(v) (\mathcal{P}_v \rho)(x) \tag{15}$$

where \mathcal{P}_v is the Perron–Frobenius operator for the translation T_v . Since T_v is quantized on \mathcal{H}_N into the unitary matrix $\hat{T}_{v^{(N)}}$, a natural way to define a quantum coarse-graining super-operator

would be through the integral

$$\int_{\mathbb{T}^2} dv K_\epsilon(v) \hat{\mathcal{P}}_{v^{(N)}}.$$

For convenience, we prefer a slightly different definition. The map $v \mapsto v^{(N)}$ is constant on squares of side $1/N$, so the above integral reduces to a finite sum over $V \in \mathbb{Z}_N^2$, with each operator $\hat{\mathcal{P}}_{V/N}$ multiplied by the average of K_ϵ over the corresponding square. K_ϵ being a smooth function, this average is semiclassically close to the value $K_\epsilon(V/N)$, therefore for N large the above integral is well approximated by the sum:

$$\hat{D}_\epsilon = \frac{F(\epsilon, N)}{N^2} \sum_{V \in \mathbb{Z}_N^2} K_\epsilon \left(\frac{V}{N} \right) \text{ad}(\hat{T}_{V/N}). \quad (16)$$

The prefactor $F(\epsilon, N)$ is needed to guarantee that \hat{D}_ϵ conserves the trace, that is $\hat{D}_\epsilon \hat{\rho}_0 = \hat{\rho}_0$. This factor is easily expressed in terms of the two-dimensional theta function:

$$\theta_K(\epsilon N, \zeta) \stackrel{\text{def}}{=} \sum_{v \in \mathbb{Z}^2} \tilde{K}(\epsilon N(v + \zeta)), \quad \zeta \in \mathbb{T}^2. \quad (17)$$

For Gaussian coarse-graining $K(x) = G(x) = e^{-\pi|x|^2}$, this function reduces to the product of two classical Jacobi one-dimensional theta functions. In the limit $\epsilon N \gg 1$, the function θ_K is peaked around the point $\zeta = 0$, due to the fast decrease of $\tilde{K}(\xi)$. Now, one easily checks that $F(\epsilon, N) = \theta_K(\epsilon N, 0)^{-1}$ converges to $\tilde{K}(0) = 1$ in the limit $\epsilon N \rightarrow \infty$.

4.2.2. Spectrum of the quantum coarse-graining operator. The spectrum of \hat{D}_ϵ on L_N^2 is as easy to analyse as that of D_ϵ (see equation (6)). Using the group relation

$$\text{ad}(\hat{T}_v) \hat{T}_{v'} = e^{-i(v \wedge v' / \hbar)} \hat{T}_{v'}, \quad (18)$$

we see that for any $k \in \mathbb{Z}_N^2$, the quantum translation $\hat{T}_{k/N}$ ($= Op_N(\rho_k)$) is an eigenstate of \hat{D}_ϵ with eigenvalue

$$d_{\epsilon, k}^{(N)} = \frac{F(\epsilon, N)}{N^2} \sum_{V \in \mathbb{Z}_N^2} K_\epsilon \left(\frac{V}{N} \right) e^{2i\pi k \wedge (V/N)} = \frac{\theta_K(\epsilon N, k/N)}{\theta_K(\epsilon N, 0)}. \quad (19)$$

For fixed k and $\epsilon N \rightarrow \infty$, one has the asymptotics $d_{\epsilon, k}^{(N)} = \tilde{K}(\epsilon k) + O((\epsilon N)^{-\alpha})$ for any power $\alpha > 0$, so that the eigenvalue of \hat{D}_ϵ associated with $\hat{T}_{k/N}$ converges to the eigenvalue of D_ϵ associated with its symbol ρ_k . The estimate is sharper in the Gaussian case:

$$\forall k \in \mathbb{Z}_N^2, \quad d_{\epsilon, k}^{(N)} = e^{-\pi \epsilon^2 k^2} + O(e^{-\pi(\epsilon N)^2/4}) \quad (20)$$

so that the relative deviations between classical and quantum eigenvalues are exponentially small, uniformly on the modes $k \in \{|k_1|, |k_2| \leq (N/2)(1 - \delta)\}$ (with $\delta > 0$ fixed). For the Gaussian case, both classical and quantum spectra are strictly positive, which is not true in general. The spectrum of \hat{D}_ϵ for a Gaussian noise is plotted in figure 1 (left).

If we replace $\tilde{K}(\xi)$ by the sharp cut-off $\Theta(1 - |\xi|)$, then $d_{\epsilon, k}^{(N)} = 1$ for $|k| < \epsilon^{-1}$, $d_{\epsilon, k}^{(N)} = 0$ otherwise: the coarse-graining truncates the expansion (11), keeping only short wavevectors (modulo N). In other words, \hat{D}_ϵ truncates the Fourier series of the polynomial Weyl symbol W_ρ^p , keeping only the coefficients $|k| < \epsilon^{-1}$.

A Fourier cut-off was also used as a definition for the quantum coarse-graining in [31], but there the cut-off was applied to the *Husimi function* of $\hat{\rho}$ instead of its polynomial Weyl symbol.

4.2.3. *Probabilistic interpretation and generalizations of coarse-graining.* In a different physical framework (one-dimensional quantum spin chains), Prosen [38] recently defined a similar quantum coarse-graining by truncating the densities on finite-dimensional spaces. In this case, the quantum densities are decomposed into sums of spin operators acting on finite sequences of spins (e.g. $\sigma_1(x)\sigma_1(x+1)\cdots\sigma_1(x+l)$). The truncation consists in keeping only those operators for which $l \leq \epsilon^{-1}$.

The right-hand side of equation (16) expresses the super-operator \hat{D}_ϵ in the *Kraus representation*, i.e. as a sum $\sum_j \text{ad}(\hat{E}_j)$, where the operators \hat{E}_j on \mathcal{H}_N satisfy the condition $\sum_j \hat{E}_j^\dagger \hat{E}_j = \text{Id}_N$. Kraus super-operators conserve the trace and the ‘complete positivity’ of density matrices [17].

The right-hand side of equations (15) and (16) may be interpreted as a *random global jump* for the density, which jumps at a distance v with a probability $\propto K_\epsilon(v)$. $D_\epsilon \rho$ and its quantum counterpart represent the average over all these random jumps. Since D_ϵ or \hat{D}_ϵ do not depend on time, they therefore represent the classical and quantum versions of a memoryless Markov process.

In a different scope, a super-operator similar to \hat{D}_ϵ was used in [33] to study the spectral correlations of the quantum map \hat{M} in the semiclassical limit. Coarse-graining was there interpreted as an average over a set of quantum maps close to identity. The phase space can be an arbitrary (quantizable) symplectic manifold, and the classical and quantum averages are generated by a finite set of Hamiltonians $\{H_j\}_{j=1,\dots,f}$; K_ϵ is a smooth probability kernel in f variables with compact support of scale ϵ around the origin. The classical and quantum coarse-graining operators are defined as:

$$\begin{aligned} D_\epsilon^{\{H_j\}} \rho(x) &= \int_{\mathbb{R}} d^f t K_\epsilon(t) \rho(\varphi_{\sum_j t_j H_j}^{-1}(x)), \\ \hat{D}_\epsilon^{\{H_j\}} \hat{\rho} &= \int_{\mathbb{R}^f} d^f t K_\epsilon(t) \text{ad}(e^{-i \sum_j \hat{H}_j t_j / \hbar}) \rho. \end{aligned} \tag{21}$$

This scheme is more general than what we have done on the torus: one does not need any group action on the phase space, but only a sufficient number of Hamiltonians. We recover our previous definition on the torus if we take for ‘Hamiltonians’ the multivalued functions $H_1 = p \bmod 1$, $H_2 = -q \bmod 1$ (these functions are not well defined on \mathbb{T}^2 , but their flows are). The qualitative spectral features of the classical coarse-grained propagator $D_\epsilon^{\{H_j\}}$ for small ϵ should not depend on the selected family of Hamiltonians $\{H_j\}$, as long as the second-order operator $\sum_{j=1}^f (\nabla_{H_j})^2$ is elliptic (in the above case on the torus, this is the Laplace operator $\partial^2/\partial q^2 + \partial^2/\partial p^2$, which is indeed elliptic) [27].

In the framework of quantum mechanics on the 2-sphere, a different type of dissipative super-operator $\hat{\mathcal{P}}_\tau = \hat{D}_\tau \circ \text{ad}(\hat{M})$ was considered in [13], where \hat{D}_τ is a quantum dissipation operator obtained by integrating a quantum *master equation* during the time τ . This dissipation operator first appeared in the study of super-radiance in atomic physics [10]. As a main difference with our noisy propagator $\hat{\mathcal{P}}_\epsilon$, the (unique) invariant eigenmode of $\hat{\mathcal{P}}_\tau$ is different from $\hat{\rho}_0$. This corresponds to the fact that the corresponding classical propagator \mathcal{P}_τ (obtained from $\hat{\mathcal{P}}_\tau$ by taking the semiclassical limit) does not leave invariant the uniform density ρ_0 , but rather a more singular measure, which may be supported either on a discrete set of points, or even on a more complicated ‘strange attractor’.

4.3. Quantum coarse-grained propagator

We will now study the quantum analogue of \mathcal{P}_ϵ , that is the coarse-grained quantum propagator $\hat{\mathcal{P}}_\epsilon = \hat{D}_\epsilon \circ \hat{\mathcal{P}}_M$. Similarly as the classical propagator, $\hat{\mathcal{P}}_\epsilon$ maps a Hermitian density to a

Hermitian density; as a result, its spectrum is symmetric with respect to the real axis. Like \hat{D}_ϵ , $\hat{\mathcal{P}}_\epsilon$ is a Kraus super-operator, and therefore realizes a quantum Markov process: the quantum density first evolves through the deterministic map $\text{ad}(\hat{M})$, then performs a random quantum jump through $\text{ad}(\hat{T}_{V/N})$, with a probability $\propto K_\epsilon(V/N)$.

Linear combinations of quantum translations were considered in [7] as models for decoherence on the quantum torus. The authors studied the evolution of densities through an operator similar to $\hat{\mathcal{P}}_\epsilon$, by computing the time evolution of the ‘purity’ $\text{tr}(\hat{\rho}^2)$. They took for \hat{M} the quantized baker’s map, which is fully chaotic, yet discontinuous on \mathbb{T}^2 . More recently, similar computations were performed for smooth nonlinear perturbations of cat maps [21].

The author of [13] uses Gutzwiller-type trace formulae to estimate the traces of powers of the dissipative quantum propagator $\text{tr}(\hat{\mathcal{P}}_\tau^n)$, in the regime of n fixed and $\hbar \rightarrow \infty$; from them he shows that each trace converges to the corresponding trace of the classical dissipative propagator $\text{tr}(\mathcal{P}_\tau^n)$ (this trace being given by a sum over periodic orbits as well).

In the following I will not use any trace formula, but more basic semiclassical and operator-theoretic techniques to compare quantum and classical coarse-grained propagators. $\hat{\mathcal{P}}_\epsilon$ is indeed spectrally similar to its classical counterpart \mathcal{P}_ϵ . It conserves the trace: $\hat{\mathcal{P}}_\epsilon \hat{\rho}_0 = \hat{\rho}_0$, but in contrast with its noiseless version $\hat{\mathcal{P}}$, it has for unique invariant density $\hat{\rho}_0$, all other eigenvalues (in number $N^2 - 1$) being inside the unit disc. As a non-classical property, $\hat{\mathcal{P}}_\epsilon$ destroys purity: the image of a pure state $\hat{\rho} = |\psi\rangle\langle\psi|$ is not a pure state.

The following theorem, which is the central result of this paper, relates more precisely the spectra of $\hat{\mathcal{P}}_\epsilon$ and \mathcal{P}_ϵ in the semiclassical limit: it states the ‘semiclassical spectral stability’ of coarse-grained propagators.

Theorem 1. *For any smooth map M on the torus and any fixed $\epsilon > 0$, the spectrum of the quantum coarse-grained propagator $\hat{\mathcal{P}}_\epsilon = \hat{D}_\epsilon \circ \hat{\mathcal{P}}_M$ on L^2_N converges in the semiclassical limit $N \rightarrow \infty$ to the spectrum of the classical coarse-grained propagator $\mathcal{P}_\epsilon = D_\epsilon \circ \mathcal{P}_M$ on $L^2(\mathbb{T}^2)$. For any $r > 0$, the convergence is uniform in the annulus $R_r = \{r \leq |\lambda| \leq 1\}$.*

To compare the classical and quantum propagators, we use the isometry between the subspace \mathcal{I}_N of $L^2(\mathbb{T}^2)$ and L^2_N , induced by the Weyl quantization Op_N and its inverse W^P (see section 4.1.1 for notation). $\hat{\mathcal{P}}_\epsilon$ is then isometric to $\sigma_N(\hat{\mathcal{P}}_\epsilon) \stackrel{\text{def}}{=} W^P \circ \hat{\mathcal{P}}_\epsilon \circ Op_N \circ \Pi_{\mathcal{I}_N}$ ($\Pi_{\mathcal{I}_N}$ projects orthogonally $L^2(\mathbb{T}^2)$ onto \mathcal{I}_N). We therefore need to compare the operators $\sigma_N(\hat{\mathcal{P}}_\epsilon)$ and \mathcal{P}_ϵ on $L^2(\mathbb{T}^2)$. The crucial semiclassical estimate is the following lemma.

Lemma 1. *The finite-rank operators $\sigma_N(\hat{\mathcal{P}}_\epsilon)$ converge to \mathcal{P}_ϵ in the operator norm on $L^2(\mathbb{T}^2)$, in the limit $N \rightarrow \infty$.*

Proof. The key semiclassical ingredient is Egorov’s property (14). From the norm inequality

$$\|\hat{\rho}\|_{\text{HS}}^2 = \frac{1}{N} \text{tr}(\hat{\rho}^\dagger \hat{\rho}) \leq \|\hat{\rho}\|_{\mathcal{L}(\mathcal{H}_N)}^2,$$

the convergence in (14) also holds for the Hilbert–Schmidt norm, that is on the space L^2_N . Using the symbol map W^P and its inverse Op_N on \mathcal{I}_N , we will convert operators on L^2_N into operators on $L^2(\mathbb{T}^2)$. We notice that for any $k \in \mathbb{Z}^2$, $\rho_k \in \mathcal{I}_N$ for large enough N . The evolved density $\mathcal{P}_M \rho_k$ is in general not in \mathcal{I}_N , but it is smooth since M is so. Any smooth density ρ is asymptotically equal to its projection on \mathcal{I}_N , so that

$$\forall \rho \in C^\infty(\mathbb{T}^2), \quad \|W^P \circ Op_N(\rho) - \rho\|_{L^2(\mathbb{T}^2)} \xrightarrow{N \rightarrow \infty} 0.$$

Using this fact, Egorov’s property can be recast into:

$$\forall k \in \mathbb{Z}^2, \quad \|\sigma_N(\hat{\mathcal{P}}_M)\rho_k - \mathcal{P}_M \rho_k\|_{L^2(\mathbb{T}^2)} \xrightarrow{N \rightarrow \infty} 0.$$

This means that the sequence of operators $\sigma_N(\hat{\mathcal{P}}_M)$ semiclassically converges to \mathcal{P}_M in the *strong topology* on $\mathcal{B}(L^2)$ (the bounded operators on $L^2(\mathbb{T}^2)$). Now, a standard lemma in functional analysis [11, lemma 2.8] states that if a sequence A_n of bounded operators on some Banach space converges strongly to the operator A , then for any compact operator K , KA_n converges to KA in the operator norm. Since D_ϵ is compact, this implies that $D_\epsilon \circ \sigma_N(\hat{\mathcal{P}}_M)$ converges to $\mathcal{P}_{\epsilon, M}$ in the operator norm. A simple comparison of the eigenvalues shows that $\|\sigma_N(\hat{D}_\epsilon) - D_\epsilon\|_{\mathcal{B}(L^2)} \rightarrow 0$ as $N \rightarrow \infty$, which achieves the proof of the lemma. \square

End of proof of the theorem. From lemma 1, one applies standard methods to show that the spectrum of $\sigma_N(\hat{\mathcal{P}}_\epsilon)$ converges to that of \mathcal{P}_ϵ , as was done in section 3.1. Namely, for any $\lambda \neq 0$ and any small disc $B(\lambda, \delta)$ around it, the spectral projectors for $\sigma_N(\hat{\mathcal{P}}_\epsilon)$ and \mathcal{P}_ϵ in that disc satisfy $\|\Pi_{B(\lambda, \delta)}^{(N)} - \Pi_{B(\lambda, \delta)}\| \rightarrow 0$ as $N \rightarrow \infty$. For small enough δ , the projector $\Pi_{B(\lambda, \delta)}$ is independent of δ and of finite rank, equal to the multiplicity of λ in the spectrum of \mathcal{P}_ϵ . The above convergence implies that $\Pi_{B(\lambda, \delta)}^{(N)}$ has the same rank for N large enough, and that the corresponding eigenspaces of \mathcal{P}_ϵ and $\sigma_N(\hat{\mathcal{P}}_\epsilon)$ are close to each other. Finally, the spectrum of $\hat{\mathcal{P}}_\epsilon$ is identical with that of $\sigma_N(\hat{\mathcal{P}}_\epsilon)$. \square

This spectral stability was noticed numerically in [31] for the kicked rotator on the 2-sphere. In their case, the coarse-graining consists in a sharp truncation of the Fourier expansion of the Husimi functions of the quantum densities, but the same arguments as above can be applied to show the spectral stability of the coarse-grained propagator in the semiclassical limit.

5. On the non-commutativity of the semiclassical versus small-noise limits

In the previous section we have described the semiclassical limit of the quantum coarse-grained propagator $\hat{\mathcal{P}}_\epsilon$ for a *fixed* coarse-graining width $\epsilon > 0$. On the other hand, section 3 was dealing with the small-noise limit $\epsilon \rightarrow 0$ for the classical propagator \mathcal{P}_ϵ .

These two limits do not commute. Indeed, for fixed $N \in \mathbb{N}$ the coarse-graining operator \hat{D}_ϵ is a finite matrix, the N^2 eigenvalues of which converge to unity as $\epsilon \rightarrow 0$ (see equation (19)). Therefore, in this limit $\|\hat{D}_\epsilon - \text{Id}_{L_N^2}\| \rightarrow 0$. For $K(x)$ of compact support, we even have $\hat{D}_\epsilon = \text{Id}_{L_N^2}$ as soon as the rescaled support $(\epsilon N)\text{Supp}(K)$ has no intersection with \mathbb{Z}_*^2 . This shows that for N fixed and ϵ decreasing to zero, $\hat{\mathcal{P}}_\epsilon$ is close to unitary on L_N^2 , uniformly with respect to the map M :

$$\forall \hat{\rho} \in L_N^2 \quad \text{s.t. } \|\hat{\rho}\|_{\text{HS}} = 1, \quad (1 - \|\hat{D}_\epsilon - \text{Id}_{L_N^2}\|) \leq \|\hat{\mathcal{P}}_\epsilon \hat{\rho}\|_{\text{HS}} \leq 1. \tag{22}$$

In contrast, there should exist a regime where $N \rightarrow \infty$ (semiclassical) and simultaneously $\epsilon = \epsilon(N) \rightarrow 0$ (vanishing noise) slowly enough, such that the eigenvalues of $\hat{\mathcal{P}}_{\epsilon(N)}$ stay close to the eigenvalues of $\mathcal{P}_{\epsilon(N)}$, and therefore behave differently according to the classical properties of M . For an Anosov map, the ‘outer’ eigenvalues (say, in some annulus R_r) will converge to the Ruelle resonances, while for an integrable map they will form dense strings touching the unit circle. Equation (22) shows that a *necessary* condition for $\hat{\mathcal{P}}_\epsilon$ to possess eigenvalues close to the origin (like \mathcal{P}_ϵ) is that the coarse-graining operator \hat{D}_ϵ itself has small eigenvalues. The smallest eigenvalues of \hat{D}_ϵ correspond to the largest wave vectors in \mathbb{Z}_N^2 , namely $|k| \sim N/2$. From the explicit expression (19), this implies the condition

$$N\epsilon(N) \gg 1. \tag{23}$$

This condition is quite obvious: it means that the scale of coarse-graining $\epsilon(N)$ must be larger than the ‘quantum scale’ $1/N = 2\pi\hbar$, that is the distance between two nearby position

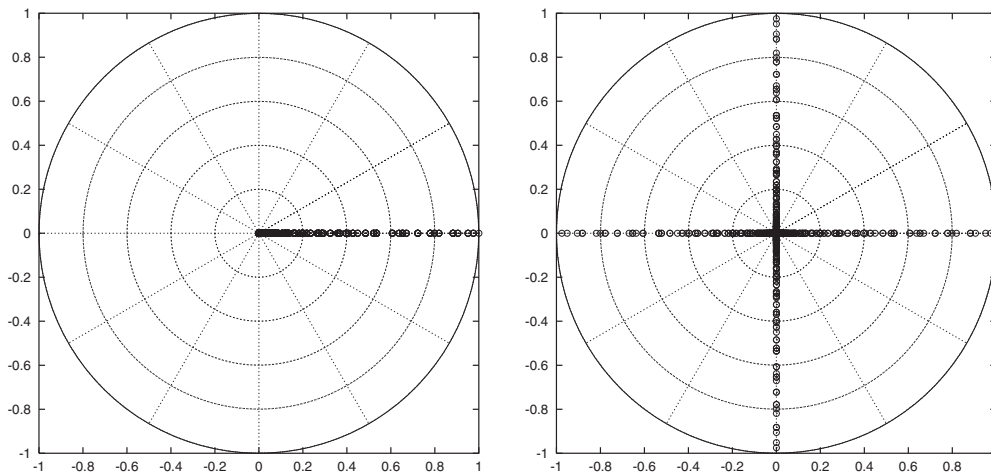


Figure 1. Spectrum of the quantum coarse-graining operator \hat{D}_ϵ for the Gaussian noise (left); spectrum of the coarse-grained $\pi/2$ -rotation $\hat{\mathcal{P}}_{\epsilon,J}$ (right). Parameters are $N = 40$, $\epsilon = N^{-1/2}$ (\circ). The large concentric circles are only shown for clarity.

states $|q_j\rangle_N$. One may wonder if this condition is sufficient, or if $\epsilon(N)$ should decrease more slowly to get the desired convergence. We have so far no definite answer to this question for a general map.

In the next two subsections, we will compare the spectra of $\hat{\mathcal{P}}_\epsilon$ and \mathcal{P}_ϵ for the various maps treated classically in sections 3.1.1 and 3.2. We know no nonlinear Anosov map for which Ruelle resonances can be computed analytically, so for this case we rely on numerical studies for the perturbed cat map [1].

We plot some numerically computed spectra, always using Gaussian noise and selecting two different \hbar -dependences for the noise width $\epsilon(N)$. We consider either a ‘slow decrease’ $\epsilon(N) = N^{-1/2}$, for which the convergence to classical eigenvalues is checked even for relatively small values of N (the largest value of N we considered is $N = 40$). To test the finer condition (26), we also consider a ‘fast decrease’ of the noise width $\epsilon(N) = \log(N)/N$, the convergence to classical eigenvalues then being harder to verify numerically.

We start by plotting in figure 1 (left) the spectrum of the quantum coarse-graining operator \hat{D}_ϵ .

5.1. Quantum linear automorphisms

In this section, we will only consider linear maps A satisfying the ‘checkerboard condition’ given in section 4.1.2, necessary for their quantization on \mathcal{H}_N . Then, the quantized linear automorphism \hat{A} satisfies the *exact* Egorov property [23]:

$$\forall k \in \mathbb{Z}^2, \quad \hat{A} \hat{T}_{k/N} \hat{A}^{-1} = \hat{T}_{Ak/N} \iff \hat{\mathcal{P}}_A Op_N(\rho_k) = Op_N(\mathcal{P}_A \rho_k) = Op_N(\rho_{Ak}).$$

The quantum propagator therefore acts as a permutation on the quantum translations, like the classical propagator on plane waves (cf equation (8)). In a first step, we treat any linear map, regardless of the nature of its dynamics.

The main difference between the quantum and classical frameworks comes from the fact that Weyl quantization Op_N is not one-to-one: $Op_N(\rho_{k+Nk'}) \propto Op_N(\rho_k)$ for any $k' \in \mathbb{Z}^2$. As a result, each orbit $O(k) = \{A^t k, t \in \mathbb{Z}\}$ has to be taken modulo \mathbb{Z}_N^2 in the quantum case, yielding a ‘quantum orbit’ $O_N(k)$ which is necessarily *finite*. Through a rescaling of $1/N$, $O_N(k)$ is

identified with a periodic orbit of the map A on the torus, situated on the ‘quantum lattice’ $((1/N)\mathbb{Z})^2$. The period $T_{N,k}$ of this orbit is the smallest $t > 0$ such that $A^t k \equiv k \pmod{\mathbb{Z}_N^2}$. To compute the spectrum of \mathcal{P}_A and $\mathcal{P}_{\epsilon,A}$ we need to analyse these quantum orbits.

The quantum orbits form a partition of \mathbb{Z}_N^2 , therefore a partition of the basis $\{\hat{T}_{k/N}, k \in \mathbb{Z}_N^2\}$ of L_N^2 . To each $O_N(k)$ corresponds the $T_{N,k}$ -dimensional subspace $\text{Span } O_N(k)$, invariant through both $\hat{\mathcal{P}}_A$ and \hat{D}_ϵ . The quantum propagator $\hat{\mathcal{P}}_A$ satisfies (we abbreviate $T_{N,k}$ with T)

$$\hat{\mathcal{P}}_A^T O p_N(\rho_k) = O p_N(\rho_{A^T k}) = O p_N(\rho_{k+NV}) = (-1)^\gamma O p_N(\rho_k) \tag{24}$$

for some $V \in \mathbb{Z}^2$, and $\gamma = k \wedge V + NV_1 V_2$. This implies that the eigenvalues of $\hat{\mathcal{P}}_A$ on $\text{Span } O_N(k)$ are the phases $\{\exp((2i\pi/T)(r + \gamma/2)), r = 0, \dots, T - 1\}$. By switching on the noise, the equation (24) is modified by inserting the action of \hat{D}_ϵ on the successive modes $\hat{T}_{A^t k/N}$. As a result,

$$\hat{\mathcal{P}}_{\epsilon,A}^T \hat{T}_{k/N} = (-1)^\gamma d_{\epsilon,O(k)}^{(N)} \hat{T}_{k/N}$$

with

$$d_{\epsilon,O(k)}^{(N)} \stackrel{\text{def}}{=} \prod_{t=0}^{T-1} d_{\epsilon,A^t k}^{(N)}.$$

The spectrum of $\hat{\mathcal{P}}_\epsilon$ on $\text{Span } O_N(k)$ thus consists in T regularly spaced points on the circle of radius $|d_{\epsilon,O(k)}^{(N)}|^{1/T}$. To estimate this radius, we take its logarithm

$$\frac{1}{T} \log |d_{\epsilon,O(k)}^{(N)}| = \frac{1}{T} \sum_{k' \in O_N(k)} \log |d_{\epsilon,k'}^{(N)}|. \tag{25}$$

According to equation (19), this quantity is the average over the periodic orbit $(1/N)O_N(k)$ of the function

$$f_K(\epsilon N, \zeta) \stackrel{\text{def}}{=} \log \left| \frac{\theta_K(\epsilon N, \zeta)}{\theta_K(\epsilon N, 0)} \right|.$$

This function is smooth in ζ except at possible logarithmic singularities if θ_K vanishes. In the Gaussian case $G(x) = e^{-\pi|x|^2}$, f_G has no singularities and admits for $\epsilon N \gg 1$ the asymptotic behaviour $f_G(\epsilon N, \zeta) \sim -\pi(\epsilon N \zeta)^2$ in the square $\{|\zeta_1| \leq \frac{1}{2}, |\zeta_2| \leq \frac{1}{2}\}$.

We have obtained an explicit relationship between the spectrum of $\hat{\mathcal{P}}_{\epsilon,A}$ and the structure of periodic orbits of A on the quantum lattice. The latter drastically differs between chaotic and integrable automorphisms, which leads to qualitatively different quantum spectra. Below, we sketch the description of these quantum orbits, respectively, for the elliptic, parabolic and hyperbolic maps. We use the notation and results of sections 3.1.1 and 3.2.2.

5.1.1. Elliptic transformation J. The quantization of the $\pi/2$ -rotation J yields the finite Fourier transform \hat{J} . The classical orbits $O(k)$ are of period 4. In general, the successive $J^j k$ are not congruent mod N , so that the quantum orbit $O_N(k)$ also has period 4. The only exception occurs for N even, $k = (N/2, N/2)$ (period 1) or $k = (0, N/2)$ (period 2). Assuming that the coarse-graining kernel has the symmetry $\tilde{K}(\xi) = \tilde{K}(J\xi)$, the eigenvalues of $\hat{\mathcal{P}}_{\epsilon,J}$ on a four-dimensional $\text{Span } O_N(k)$ are $\{i^l d_{\epsilon,k}^{(N)}, l = 0, \dots, 3\}$. Taking all quantum orbits into account, the spectrum forms four strings as in the classical case (see figure 1, right). For a Gaussian noise, equation (20) shows that these eigenvalues are exponentially close to the corresponding classical eigenvalues.

5.1.2. *Parabolic linear shear S.* We can quantize on \mathcal{H}_N the parabolic shear S described in section 3.2.2 if the integer s is even. Quantizing the space of \mathcal{P}_S -invariants $V_{\text{inv}} = \text{Span}\{\rho_{(l,0)}, l \in \mathbb{Z}\}$ leads to the $\hat{\mathcal{P}}_S$ -invariants $V_{\text{inv},N} = \text{Span}\{\hat{T}_{(l/N,0)}, l \in \mathbb{Z}_N\}$. Each $\hat{T}_{(l/N,0)}$ is an eigenstate of $\hat{\mathcal{P}}_\epsilon$ with eigenvalue $d_{\epsilon,(0,l)}^{(N)}$, which is close to the classical eigenvalue $\tilde{K}(\epsilon(0,l))$ for $\epsilon N \gg 1$; these eigenvalues then form a string connecting unity to the origin.

Now we study the spectrum of $\hat{\mathcal{P}}_\epsilon$ on the orthogonal of the invariant space, $V_{\text{inv},N}^\perp$. For $k = (k_1, k_2)$ with $k_2 \not\equiv 0 \pmod N$, the infinite orbit $O(k) = \{k + (jsk_2, 0), j \in \mathbb{Z}\}$ projects modulo N onto a finite orbit $O_N(k)$ whose period depends on the ‘step’ $g \stackrel{\text{def}}{=} \text{gcd}(N, sk_2)$: $O_N(k) = \{(k_1 + jg \pmod N, k_2) \mid j = 0, \dots, N/g - 1\}$. For a fixed $k_2 \in \mathbb{Z}_*$, the step g stays bounded in the limit of large N , so that the sum (25) behaves as the integral $\int_0^1 dt f_K(\epsilon N, (t, k_2/N))$; for the Gaussian noise, the latter yields $-\pi\epsilon^2(N^2/12 + k_2^2) + O(1)$. For a general value of $k_2 \in \mathbb{Z}_N \setminus \{0\}$, the step g may be of order N , in which case the sum (25) is not well-approximated by an integral; still, one can (for Gaussian noise) prove the uniform upper bound:

$$\frac{1}{T_{N,k}} \log |d_{\epsilon,O(k)}^{(N)}| \leq -C(\epsilon N)^2$$

with $C = \pi \min\{1/s^2, \frac{1}{16}\}$. The eigenvalues of $\hat{\mathcal{P}}_\epsilon$ on $V_{\text{inv},N}^\perp$ are therefore situated on circles of radii $\leq e^{-C(\epsilon N)^2}$, so they uniformly converge to zero as $\epsilon N \rightarrow \infty$ (we recall that the spectrum of $\mathcal{P}_{\epsilon,S}$ restricted to V_{inv}^\perp reduces to $\{0\}$).

In figure 2 we show the spectra of $\hat{\mathcal{P}}_{\epsilon,S_2}$ for the linear shear $S_2 = \begin{pmatrix} 1 & 2 \\ 0 & 1 \end{pmatrix}$ and a ‘fast decreasing noise’, together with the eigenvalues $\{d_{\epsilon,(j,0)}^{(N)}\}_{j=0}^N$. The ‘non-invariant spectrum’ converges slowly to the origin, while the ‘invariant spectrum’ becomes dense on the interval $[0, 1]$. Had we chosen a larger noise width, the non-invariant spectrum would be contained in a smaller disc for the same values of N .

5.1.3. *Hyperbolic transformations.* The space of invariant densities for a hyperbolic automorphism A reduces to $V_{\text{inv}} = \mathbb{C}\rho_0$. Its orthogonal $V_{\text{inv}}^\perp = L_0^2$ is quantized into the space $L_{0,N}^2$ of traceless densities. We recall (cf section 3.1.1) that the spectrum of $\mathcal{P}_{\epsilon,A}$ on this subspace reduces to $\{0\}$, for any $\epsilon > 0$.

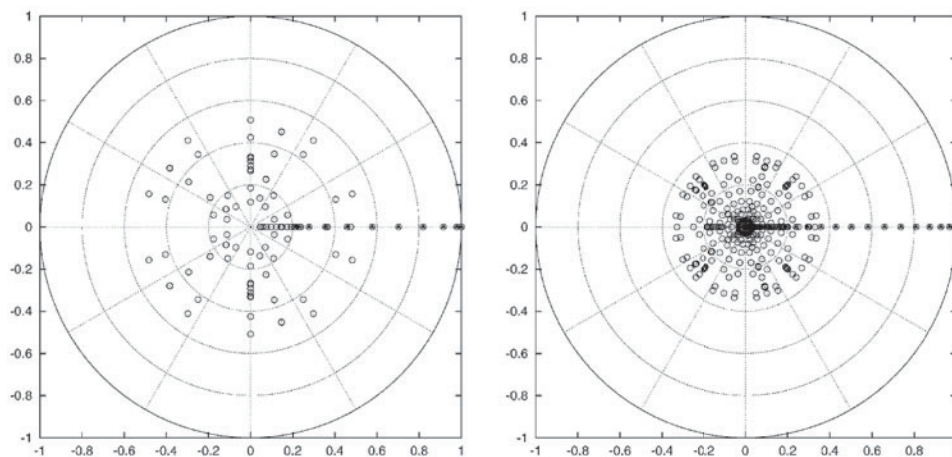


Figure 2. Spectrum of $\hat{\mathcal{P}}_{\epsilon,S_2}$ for the linear shear S_2 (○) and values $\{d_{\epsilon,(j,0)}^{(N)}\}_{j=0}^N$ (▲). Parameters are $N = 20$ (left), $N = 40$ (right) and in both cases $\epsilon = \log(N)/N$.

The periodic orbits of a hyperbolic automorphism A were thoroughly studied in [37]; the authors classified the orbits according to the $1/N$ sublattice they belong to. Yet, they gave no equidistribution estimate on long periodic orbits. Our aim is to estimate the right-hand side of equation (25) for all quantum orbits, at least for large enough N (we will restrict ourselves to the Gaussian coarse-graining). For any Anosov map, the long periodic orbits equidistribute in the statistical sense (averaging over all orbits of a given period) in the limit of long periods [36]. For a certain class of hyperbolic automorphisms, semiclassical equidistribution of all quantum orbits was obtained for an infinite subsequence of values of N [19]. Equidistribution morally implies that the sum (25) behaves as the integral

$$\int_{\mathbb{T}^2} dx f_G(\epsilon N, x) \approx \frac{\pi(\epsilon N)^2}{6}.$$

One can indeed show that for N in this subsequence, any eigenvalue λ of $\hat{\mathcal{P}}_{\epsilon,A}$ on the subspace $L^2_{0,N}$ satisfies

$$|\lambda| \leq \exp \left\{ -\frac{\pi(\epsilon N)^2}{6} + O(\epsilon^2 N^{3/2}) \right\}.$$

There also exist arbitrary large values of N for which the period $T(N)$ of A modulo N is as small as $2 \log N / \lambda + O(1)$, where $\lambda > 0$ is the Lyapounov exponent of A [37]. All quantum orbits $O_N(k)$ have periods dividing $T(N)$. Starting from $k_0 = (0, 1)$, the linear dynamics shows that the point $A^t k_0 / N$ remains close to the origin (i.e. at a distance $\ll 1$) along the unstable direction until the time $\approx (\log N) / \lambda$, when it reaches the boundary of the square $\{|\zeta_1| \leq \frac{1}{2}, |\zeta_2| \leq \frac{1}{2}\}$; it is then straight away ‘captured’ by the stable manifold, which brings it back to the origin during the remaining $\approx (\log N) / \lambda$ steps. This orbit thus achieves an ‘optimally short’ homoclinic excursion from the unstable origin, and is far from being equidistributed. The average of f_G along this orbit is of order $-C(\epsilon N)^2 / \log N$, so the eigenvalues of $\hat{\mathcal{P}}_{\epsilon,A}$ on $\text{Span } O_N(k_0)$ have a radius $\approx \exp(-C(\epsilon N)^2 / \log N)$. These eigenvalues will therefore semiclassically converge to zero under the condition

$$\frac{\epsilon N}{\sqrt{\log N}} \rightarrow \infty. \tag{26}$$

We believe that these particular values of N represent the ‘worst case’ as far as equidistribution of long orbits is concerned, and that condition (26) suffices for the spectra of $\hat{\mathcal{P}}_{\epsilon,A}|_{L^2_{0,N}}$ to semiclassically converge to zero for the full sequence $N \in \mathbb{N}$. In figure 3 we show the spectrum of $\hat{\mathcal{P}}_{\epsilon,A_0}$ for the quantization of the cat map $A_0 = \begin{pmatrix} 2 & 1 \\ 3 & 2 \end{pmatrix}$, with fast decreasing noise width.

Remark. For both the parabolic and the hyperbolic automorphisms, the spectrum of $\hat{\mathcal{P}}_\epsilon$ on $V_{\text{inv},N}^\perp$ reduces to $\{0\}$ if the coarse-graining consists in a sharp truncation in Fourier space, and ϵ^{-1} grows as $\epsilon^{-1} \approx cN$ with c a finite but small constant (depending on the classical map). Any non-trivial quantum orbit $O_N(k_0)$ then contains an element k s.t. $|k| > \epsilon^{-1}$, such that the corresponding mode $\hat{T}_{k/N}$ is killed by \hat{D}_ϵ .

5.1.4. Quantum translations. As we mentioned in section 4.1.2, any classical translation T_v with $v \in \mathbb{T}^2$ can be quantized on \mathcal{H}_N by the quantum translation $\hat{T}_{v^{(N)}}$, where $v^{(N)}$ is the ‘closest’ point to v on the quantum lattice. This quantization was shown [32] to satisfy Egorov’s property (14).

From equation (18), the quantum propagator $\hat{\mathcal{P}}_{v^{(N)}} = \text{ad}(\hat{T}_{v^{(N)}})$ admits any quantum translation $\hat{T}_{k/N} = Op_N(\rho_k)$ as an eigenstate, with eigenvalue $e^{-2i\pi v^{(N)} \wedge k}$. All eigenvalues

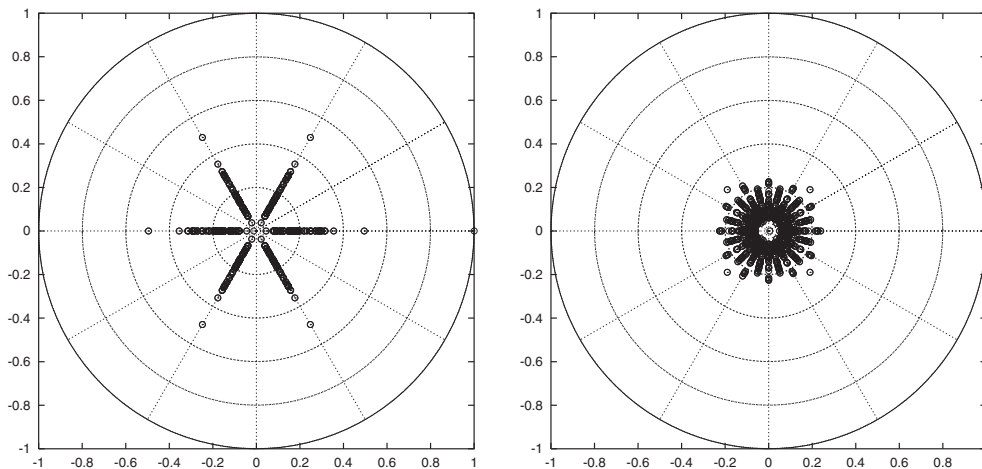


Figure 3. Spectrum of $\hat{\mathcal{P}}_{\epsilon, A_0}$ for the cat map A_0 . Parameters are $N = 30$ (left), $N = 40$ (right) and in both cases $\epsilon = \log(N)/N$. $N = 30$ corresponds to a ‘short quantum period’ $T(30) = 6$, which is clearly visible in the shape of the spectrum.

are N th roots of unity, and are at least N -degenerate; in the case the classical translation T_v is ergodic, these degeneracies contrast with the non-degenerate (but dense) spectrum of \mathcal{P}_v . In contrast, for a rational translation (the classical eigenvalues form a finite set), the quantum eigenvalues may take values in all N th roots of unity, in the case N and $v^{(N)}$ are coprime. The spectra of \mathcal{P}_v and $\hat{\mathcal{P}}_{v^{(N)}}$ may thus be qualitatively very different.

This difference disappears when one switches on the noise. Each $\hat{T}_{k/N}$ is also an eigenstate of the coarse-grained propagator $\hat{\mathcal{P}}_{\epsilon, v} = \hat{D}_\epsilon \hat{\mathcal{P}}_{v^{(N)}}$, associated with the eigenvalue $e^{2i\pi k \wedge v^{(N)}} d_{\epsilon, k}^{(N)}$. In the semiclassical limit, the deviation from the corresponding classical eigenvalue $e^{2i\pi k \wedge v} \tilde{K}(\epsilon k)$ (cf section 3.2.1) depends on both the wavevector k and the difference $v - v^{(N)}$.

To give an example, the rational translation vector $v = (0, \frac{1}{3})$ leads to three eigenvalues $e^{2i\pi l/3}$ for the classical propagator \mathcal{P}_v , and three (infinite) strings for the spectrum of $\mathcal{P}_{v, \epsilon}$. Quantum-mechanically, if N is a multiple of 3 one takes $v^{(N)} = v$, and the eigenvalues of $\hat{\mathcal{P}}_{v, \epsilon}$ are exponentially close to the classical ones (figure 4, left). In the case $N = 3n + 1$, the quantum translation vector will be $v^{(N)} = (0, n/(3n + 1))$, so that the classical and quantum noiseless eigenvalues for the mode ρ_k deviate by an angle $2\pi k \wedge (v - v^{(N)}) = 2\pi k_1/3N$: this deviation can be as large as $\pi/3$ for wavevectors $|k_1| \approx N/2$. After switching on the noise, the classical and quantum eigenvalues for $k \in \mathbb{Z}_N^2$ can deviate by at most $O(1/\epsilon N)$, the maximal deviations occurring for wavevectors $|k_1| \simeq \epsilon^{-1}$, $k_2 = O(1)$ (figure 4, centre).

5.2. Examples of quantized nonlinear maps

In this section we shortly review the spectrum of quantized coarse-grained propagators for three nonlinear maps: we first treat the nonlinear parabolic shear of section 3.2.3 and the stroboscopic map of the Harper Hamiltonian (section 3.2.4), for which we have some analytic handle. We then consider a perturbation of the cat map A_0 and compare the numerically computed eigenvalues of $\hat{\mathcal{P}}_\epsilon$ to the spectrum of \mathcal{P}_ϵ obtained in [1].

(a) The nonlinear shear described in section 3.2.3 is quantized by taking the product of the quantum linear shear \hat{S} (see section 5.1.2) with the matrix $e^{-i\hat{F}/\hbar}$. Since $F(p)$ is a function of

the impulsion only, its Weyl quantization \hat{F} acts diagonally on the impulsion basis $\{|p_j\rangle\}$. As a result, the perturbation $\text{ad}(e^{-i\hat{F}/\hbar})$ acts trivially on any projector $|p_j\rangle\langle p_j|$, and therefore on any translation $\hat{T}_{(0,m)/N}$. As a result, the spectrum of the noisy nonlinear propagator on $V_{\text{inv},N}$ forms the same string as for the linear shear.

The action of $\hat{\mathcal{P}}$ on $V_{\text{inv},N}^\perp$ can be studied as in the classical case: the propagator acts inside each subspace $V_{n,N} = \text{Span}\{\hat{T}_{(n,m)/N}, m \in \mathbb{Z}_N\}$, as a unitary $N \times N$ Toeplitz matrix $\hat{\mathcal{P}}^{(n)}$ (instead of a simple permutation). In appendix A.2 we study the non-unitary spectrum of $\hat{\mathcal{P}}_\epsilon^{(n)}$ when taking for $\tilde{K}(\xi)$ a sharp cut-off: $\hat{\mathcal{P}}_\epsilon^{(n)}$ is then the truncation of $\hat{\mathcal{P}}^{(n)}$ to the subspace $\{|m| \leq \epsilon^{-1}\}$. We compare this truncated propagator with the corresponding classical one, and show that if $\epsilon N \gg 1$, both spectra belong to the same union of one-dimensional strings contained in a fixed ‘small’ disc around the origin, the size of which depends on the strength of the perturbation F' . The spectrum of $\hat{\mathcal{P}}$ for the quantized nonlinear shear $e^{-i\hat{F}/\hbar}\hat{S}_2$ with $\hat{F} = (0.25/2\pi)\cos(2\pi\hat{p})$ is shown in figure 5 (left) for $N = 40$ and $\epsilon = \log(N)/N$, together with the values $\{d_{\epsilon,(j,0)}^{(N)}\}_{j=0}^N$.

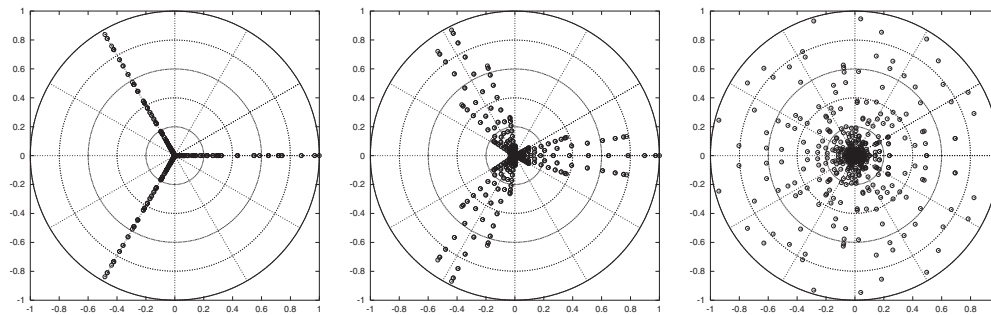


Figure 4. Spectrum of $\hat{\mathcal{P}}_{\epsilon,v}$ for the translations $v = (0, \frac{1}{3})$ (left: $N = 30$, centre: $N = 37$) and $v = (1/\sqrt{2}, 1/\sqrt{5})$ (right: $N = 37$). The noise strength is $\epsilon = N^{-1/2}$. For the rational translation, the eigenvalues are either exactly on the classical axes (for N a multiple of 3), or semiclassically converge to it. For the irrational one, the eigenvalues become dense in the full disc.

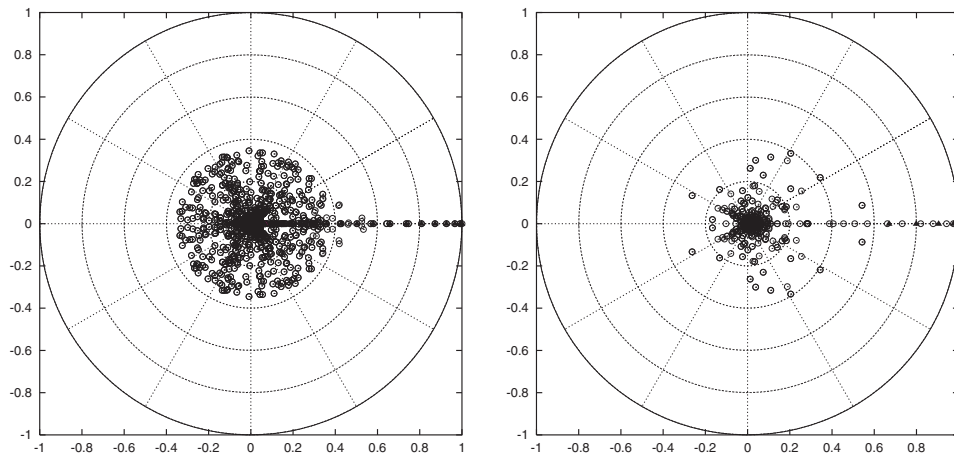


Figure 5. Spectrum of $\hat{\mathcal{P}}_\epsilon$ for the nonlinear shear $e^{-i\hat{F}/\hbar}\hat{S}_2$ (left: $N = 40$, $\epsilon = \log(N)/N$) and the Harper map $e^{-i\hat{H}/\hbar}$ (right: $N = 40$, $\epsilon = N^{-1/2}$). In both cases we also plotted some values $d_{\epsilon,(j,0)}^{(N)}$ (\blacktriangle).

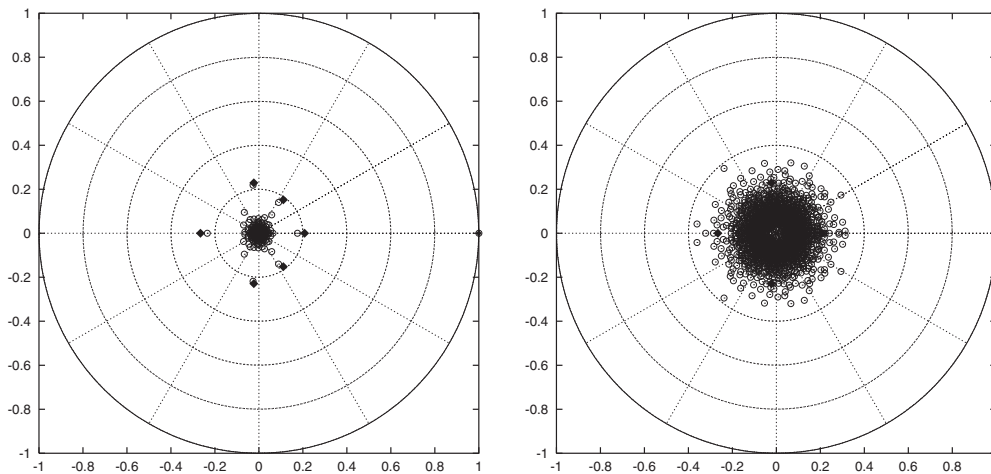


Figure 6. Spectrum of $\hat{\mathcal{P}}_\epsilon$ for the quantum perturbed cat map \hat{A}_{nl} (○) together with the largest seven classical resonances (◆). Left: $N = 40$, $\epsilon = N^{-1/2}$. Right: $N = 40$, $\epsilon = \log(N)/N$.

(b) The quantization of the stroboscopic map φ_H^1 for the Harper flow, i.e. the unitary matrix $e^{-i\hat{H}/\hbar}$, leads to the propagator $\hat{\mathcal{P}}_H$ leaving invariant any density of the type \hat{H}^n . Under the same conditions for the coarse-graining kernel $\tilde{K}(\xi)$ as in the classical case (see section 3.2.4), $\hat{\mathcal{P}}_{H,\epsilon}$ may admit for eigenstates \hat{H} , $(\hat{H}^2 - \text{Id})$ and $(\hat{H}^3 - (7 + 2\cos(2\pi/N)/4)\hat{H})$, and the associated eigenvalues $\{d_{\epsilon,(j,0)}^{(N)}\}_{j=1}^3$ converge to the classical eigenvalues $\{\tilde{k}(j\epsilon)\}_{j=1}^3$ if $\epsilon N \rightarrow \infty$. The spectrum of $\hat{\mathcal{P}}_{H,\epsilon}$ for $N = 40$ and $\epsilon = N^{-1/2}$ is shown in figure 5 (right), together with the values $\{d_{\epsilon,(j,0)}^{(N)}\}_{j=0}^4$. For the Gaussian kernel used there, only \hat{H} is an eigenstate of $\hat{\mathcal{D}}_\epsilon$, so the subsequent eigenvalues are hybridized by the coarse-graining. A ‘string’ of eigenvalues along the positive real axis is clearly visible on the plot.

(c) We consider the quantization of the perturbed cat map studied in [1], that is the map

$$A_{\text{nl}} : \begin{pmatrix} q \\ p \end{pmatrix} \mapsto \begin{pmatrix} 2q + p \\ 3q + 2p + \kappa(\cos(2\pi q) - \cos(4\pi q)) \end{pmatrix}.$$

We selected the perturbation $\kappa = 0.5/2\pi$ in order to compare the quantum spectrum with the classical resonance spectrum described in [1, figure 2]. In figure 6 we plot the spectrum of $\hat{\mathcal{P}}_\epsilon$ for $N = 40$ together with the seven ‘outer’ resonances whose values are given in [1, table 1]. In the ‘large noise’ regime (left), the largest quantum eigenvalues are indeed close to these resonances, and the rest of the spectrum is inside a smaller disc. The small-noise regime (right) does not uncover the classical resonances, however the non-invariant spectrum is already contained in a relatively small disc around the origin, of radius comparable with the largest resonance.

5.3. Concluding remarks

In spite of the relatively low values of N used in the numerical plots, one can already clearly distinguish two different types of behaviour of the quantum spectra, depending on the classical motion, especially for the slow noise decrease $\epsilon = N^{-1/2}$. For the integrable maps, the largest non-trivial eigenvalue of the noisy quantum propagator $\hat{\mathcal{P}}_\epsilon$ is at a distance ϵ^2 from unity, and this eigenvalue is the first one of a string of eigenvalues connecting unity with a neighbourhood of zero. In contrast, for the two chaotic maps we studied (linear and perturbed cat maps), the

spectrum already shows a finite gap for these values of N , even in the fast-decreasing noise regime $\epsilon = \log(N)/N$; however, for the relatively low values of N shown in the plots, the gap is governed by the classical resonances only in the regime of larger noise $\epsilon = N^{-1/2}$. I conjecture that the quantum spectrum also converges to the classical spectrum (in any annulus R_r) in the regime $\epsilon = \log(N)/N$, this being visible only for much higher values of N .

6. General conclusion

In this paper we have shown the connection between the spectra of coarse-grained quantum and classical propagators for maps on the two-dimensional torus. I claim that theorem 1 can be straightforwardly extended to maps on any compact phase space, like the 2-sphere S^2 used in [31, 26]. Using our knowledge of the spectrum of the classical noisy map, one infers the presence or the absence of a *finite gap* between the (trivial) eigenvalue unity on the one hand, the rest of the spectrum on the other hand, taking both the semiclassical ($\hbar \rightarrow 0$) and small-noise ($\epsilon \rightarrow 0$) limits in a well-defined way. The presence of this gap in the classical noisy propagator is related to the ergodic properties of the map. At one extreme, corresponding to integrable maps with infinitely many invariant densities, there is no gap in the small-noise limit, and the spectrum contains a dense ‘string’ of eigenvalues connecting unity with the interior of the disc: the long-time evolution is therefore governed by the eigenmodes associated with these large eigenvalues, and is typically of *diffusive type*. At the opposite extreme, for an Anosov map (‘strongly chaotic’), the spectrum exhibits a finite gap, responsible for the (classical) exponential mixing. The case of maps with less chaotic behaviour is far from being settled. The example of irrational translations shows that ergodicity does not imply the presence of a gap. Exponential mixing was recently proven for some non-uniformly or partially hyperbolic maps (see [4] for a review of recent results), which should (?) imply a gap in the spectrum of \mathcal{P}_ϵ . Maps with *subexponential* mixing would also deserve to be studied from this point of view. The more general case of maps with *mixed dynamics* (where the phase space can be divided between ‘regular islands’ and a ‘chaotic sea’) was mostly investigated numerically [26, 31]; one found the presence of both ‘dense strings’ of eigenvalues and isolated resonances in the spectrum of \mathcal{P}_ϵ . This (physically relevant) type of dynamics certainly deserves further study.

As in the classical framework, the presence of a gap in the spectrum of the quantum noisy propagator allows us to describe the long-time dynamics of densities induced by this propagator: $\hat{\rho}(t) = (\hat{\mathcal{P}}_\epsilon)^t \hat{\rho}(0)$. This dynamics is a possible model for a dissipative perturbation of the unitary evolution $\rho \mapsto M^t \rho M^{-t}$, the dissipation being induced by the interaction with the environment [7]. One measure of the decoherence occurring through this evolution is the ‘purity’ $\text{tr}(\hat{\rho}(t))^2$. For an Anosov map M , the long-time evolution of this quantity will be governed by the largest non-trivial eigenvalues of \mathcal{P}_ϵ , which are semiclassically close to the classical resonances. This very evolution was recently studied for perturbed quantum cat maps, providing an estimate of the largest eigenvalues of $\hat{\mathcal{P}}_\epsilon$ for large values of N [21]. Another way to characterize the time evolution of \mathcal{P}_ϵ is through the *dissipation time* $t_{\text{diss}} = \inf\{t \in \mathbb{N} / \|\mathcal{P}_\epsilon^t\|_{B(L_0^2)} < e^{-1}\}$. In the case of linear automorphisms on the d -dimensional torus, the small-noise behaviour of t_{diss} has been shown to qualitatively depend on the dynamics [20]. The same conclusion should apply to nonlinear maps as well.

Our noise operator consists in an average over random translations in phase space. To diagonalize this operator, we have used the fact that the classical (respectively, quantum) propagators for translations \mathcal{P}_v (respectively, $\hat{\mathcal{P}}_v$) form a commutative algebra, and admit as eigenfunctions the Fourier modes. We obtained explicit expressions for the spectrum of $\mathcal{P}_{\epsilon, M}$ for the class of linear maps M , because these maps acted simply on these Fourier modes. However, as noticed in section 4.2.3, one may be interested in a more general type of diffusion

operator, like the one defined in equation (21). The spectrum of $D_\epsilon^{\{H_j\}} \circ \mathcal{P}_M$ for a given map M should be qualitatively independent of the family of Hamiltonians $\{H_j\}$, as long as the operator $D_\epsilon^{\{H_j\}}$ has the same characteristics as the coarse-graining D_ϵ , namely it leaves almost invariant some ‘soft modes’, while killing fast-oscillating modes. In particular, for M an Anosov map, the outer spectrum of $D_\epsilon^{\{H_j\}} \circ \mathcal{P}_M$ should converge to the set of resonances $\{\lambda_i\}$, and the rest is contained in a smaller disc, in the limit $\epsilon \rightarrow 0$. For an integrable map, the eigenvalues will not pointwise converge to those of $\hat{D}_\epsilon \hat{\mathcal{P}}_M$, but they should also accumulate along a ‘string’ touching unity.

Our choice for the super-operator \hat{D}_ϵ was inspired by its classical analogue, as well as its relevance to modelize the ‘quantum noise’. However, in some quantum systems experiencing (weak) interaction with the environment, the effective ‘noise’ or ‘decoherence’ superoperator may have no obvious classical analogue; this seems to be the case for instance in nuclear magnetic resonance experiments aiming at realizing a ‘quantum computer’ [15]. The quantum Hilbert space is composed of a sequence of n spins, so it is isomorphic with the torus Hilbert space \mathcal{H}_N for $N = 2^n$ (each spin corresponds to a binary digit of the position q_j). The decoherence operator acting on such a system (for a small number of spins) has been experimentally measured, it resembles the product of operators acting independently on the individual spins, and therefore does not enter in the family of diffusion operators described in this paper; in particular, such a decoherence operator seems to have no obvious classical counterpart. Conjugating this type of decoherence operator with a unitary evolution (typically, the finite Fourier transform \hat{J}) may lead to a drastically different spectrum from the one shown in figure 1 (right), not excluding the presence of a gap.

Acknowledgments

I thank M Zirnbauer and the Institut für theoretische Physik, Universität zu Köln, where this work was initiated. I am grateful to V Baladi and S De Bièvre for respectively pointing out [8, 20] to me, and thank S Keppeler for his insight on integrable maps. I had interesting discussions on the whole subject with M Saraceno and I Garcia Mata.

Appendix A

Appendix A.1. Classical nonlinear shear: spectrum of truncated Toeplitz matrices

This appendix describes the spectrum of the noisy classical propagator for a nonlinear shear (section 3.2.3). In each invariant subspace $V_n = \{e^{2i\pi nq} \rho(p)\}$ ($n \in \mathbb{Z}^*$), the Perron–Frobenius operator \mathcal{P} acts as a multiplication of the function $\rho(p)$ on the circle $\mathbb{T}^1 \ni t = e^{2i\pi p}$ by

$$a_n(e^{2i\pi p}) \stackrel{\text{def}}{=} e^{-2i\pi n(sp+F'(p))} = \sum_{m \in \mathbb{Z}} \tilde{a}_n(m) e^{2i\pi mp}. \quad (27)$$

Note that $a_n(t) = (a_1(t))^n$. In the Fourier basis, this multiplication has the form of an infinite Laurent matrix $L(a_n)$, with entries $L(a_n)_{ij} = \tilde{a}_n(i - j)$. From standard results, the spectrum of $\mathcal{P}|_{V_n}$ is absolutely continuous, with support in the range of the function $a_n(t)$ (here, the unit circle).

We consider the coarse-graining consisting in a sharp truncation in Fourier space: $\tilde{K}(\xi) = \Theta(\xi_1)\Theta(\xi_2)$. The noisy propagator \mathcal{P}_ϵ then acts on V_n as the matrix $L(a_n)$ truncated to the block $\{|m|, |m'| \leq \epsilon^{-1}\}$, or equivalently as $\{1 \leq m, m' \leq 2\epsilon^{-1} + 1\}$. We assume that the smooth function $a_n(t)$ on \mathbb{T}^1 can be continued to an analytic (or meromorphic) function on \mathbb{C}^* (for the linear shear, one has $a_n(z) = z^{-sn}$). Then, for any $r > 0$ and any $\epsilon > 0$,

the spectrum of this truncated matrix is contained in the convex hull of the curve $a_n(r\mathbb{T}^1)$ [11, proposition 2.17 and section 5.8]. For the linear shear, these curves are the circles centred at the origin, so the spectrum reduces to $\{0\}$, as expected. If the perturbation F' is small, these curves are deformations of circles, some of which remain in a small neighbourhood of the origin. As a concrete example, the perturbation $F(p) = (\alpha/2\pi) \cos(2\pi p)$ leads to the function $a_{-1}(z) = z^s \exp\{\pi\alpha(1/z - z)\}$. The curves $a_{-1}(r\mathbb{T}^1)$ satisfy

$$\forall r > 0, \quad |z| = r \implies |a_{-1}(z)| \leq r^s \exp\left(\pi\alpha \left| \frac{1}{r} - r \right|\right).$$

We assume that $s > 0$. For a small perturbation ($\alpha \ll 1$), the function on the right-hand side has a minimum of value $a_{\min}(\alpha) \lesssim (\pi\alpha e/s)^s$. This implies that for any n , the spectrum of $\mathcal{P}_{\epsilon|V_n}$ is contained in the disc of radius $(a_{\min}(\alpha))^{|n|}$ for any $\epsilon > 0$ (we have used the symmetry $a_{-n} = \bar{a}_n$).

For a more general perturbation $2\pi F'(t) = \sum_{m \geq 1} f_m t^m + \text{c.c.}$ one can use the bound $2\pi |\Im F'(rt)| \leq \sup(g(r), g(1/r))$ with $g(r) \stackrel{\text{def}}{=} \sum_{m \geq 1} |f_m| r^m$. If $g(r)$ is ‘small’, then the function $r^s \exp(g(1/r))$ has a minimum $a_{\min} \ll 1$ on \mathbb{R}_+^* . This implies that the spectrum of $\mathcal{P}_{\epsilon|V_n}$ is contained, for any ϵ , in the disc around the origin of radius $a_{\min}^{|n|}$.

Appendix A.2. Quantum nonlinear shear

The results of the previous appendix can be easily adapted to the quantized nonlinear shear. The latter is defined as the composition of the quantum linear shear \hat{S} with the Floquet operator corresponding to the Hamiltonian \hat{F} (see section 3.2.3): the quantum map reads $\hat{S}e^{-2i\pi N \hat{F}}$. Its action is diagonal in the impulsion basis $\{|p_j\rangle_N\}$ of \mathcal{H}_N ($p_j = j/N$, with $j \in \mathbb{Z}_N$):

$$\hat{S}e^{-i\hat{F}/\hbar} |p_j\rangle_N = e^{-2i\pi N((s/2)p_j^2 + F(p_j))} |p_j\rangle_N.$$

Since s is even, this expression is well defined for any $j \in \mathbb{Z}_N$. As we now show, it allows us to express the action of the propagator $\hat{\mathcal{P}}$ on the quantum translations $\hat{T}_{k/N}$. Taking $k = (m, n) \in \mathbb{Z}_N^2$, this translation can be decomposed as

$$\hat{T}_{k/N} = \sum_{j \in \mathbb{Z}_N} |p_{j+n}\rangle \langle p_j| e^{-2i\pi m(p_j+n/2N)}.$$

$\hat{\mathcal{P}}$ acts inside each subspace $V_{n,N} = \text{Span}\{\hat{T}_{(m,n)/N}, m \in \mathbb{Z}_N\} = \text{Span}\{|p_{j+n}\rangle \langle p_j|, j \in \mathbb{Z}_N\}$. The propagator $\hat{\mathcal{P}}$ indeed multiplies each $|p_{j+n}\rangle \langle p_j|$ by the phase $A_{n,N}(e^{2i\pi(p_j+n/2N)})$, with the function $A_{n,N}$ on \mathbb{T}^1 defined as:

$$A_{n,N}(e^{2i\pi p}) \stackrel{\text{def}}{=} e^{-2i\pi s n p} e^{-2i\pi N[F(p+n/2N) - F(p-n/2N)]} = \sum_{m \in \mathbb{Z}} \tilde{A}_{n,N}(m) e^{2i\pi m p}.$$

$A_{n,N}(t)$ uniformly converges to the function $a_n(t)$ of equation (27) in the limit $N \rightarrow \infty$. For our example $F(p) = (\alpha/2\pi) \cos(2\pi p)$, it takes the concise form

$$A_{n,N}(e^{2i\pi p}) = e^{-2i\pi n(sp - \alpha_{n,N} \sin(2\pi p))}$$

with

$$\alpha_{n,N} = \alpha \frac{N}{\pi n} \sin\left(\frac{\pi n}{N}\right) = \alpha \left(1 + \mathcal{O}\left(\left(\frac{n}{N}\right)^2\right)\right).$$

From there, we can express the action of $\hat{\mathcal{P}}$ on the quantum translations:

$$\hat{\mathcal{P}}\hat{T}_{(m,n)/N} = \sum_{l \in \mathbb{Z}} \hat{T}_{(m-l,n)/N} \tilde{A}_{n,N}(l) = \sum_{l \in \mathbb{Z}_N} \hat{T}_{(l,n)/N} \tilde{A}'_{n,N}(m-l)$$

where $\tilde{A}'_{n,N}(m) = \sum_{\nu \in \mathbb{Z}} (-1)^{\nu} \tilde{A}_{n,N}(m + \nu N)$. Therefore, $\hat{\mathcal{P}}$ acts on $V_{n,N}$ through the $N \times N$ Toeplitz matrix with coefficients $\tilde{A}'_{n,N}(m)$. If we truncate this matrix to the size $\{|l|, |l'| \leq \epsilon^{-1}\}$ with $\epsilon^{-1} \ll N$, we only take into account the coefficients with $|m| \leq 2\epsilon^{-1}$. Since $A_{n,N}$ is a smooth function, each of these coefficients is the sum of a ‘dominant’ term $\tilde{A}_{n,N}(m)$ and a ‘remainder’. For our example, the classical coefficients are given by Bessel functions: $\tilde{a}_n(m) = J_{m+sn}(2\pi n\alpha)$, and the same for $\tilde{A}_{n,N}(m)$, replacing α by $\alpha_{n,N}$. These coefficients therefore satisfy $|\tilde{A}_{n,N}(m)| \leq C((n\alpha)^{|m+ns|}/|m+ns|!)$, so that the remainder is uniformly bounded above by $(C'\alpha/\epsilon N)^{N/2}$ for large N . If we call $\hat{\mathcal{P}}_{\epsilon|V_{n,N}}^{\sharp}$ the truncated Toeplitz matrix with coefficients $\tilde{A}_{n,N}(m)$, we get the estimate:

$$\|\hat{\mathcal{P}}_{\epsilon|V_{n,N}} - \hat{\mathcal{P}}_{\epsilon|V_{n,N}}^{\sharp}\| \leq (2\epsilon^{-1} + 1) \left(\frac{C'\alpha}{\epsilon N}\right)^{N/2}.$$

This estimate implies that the spectra of both matrices cannot be at a distance larger than $O((\epsilon N)^{-\epsilon N/4})$. The matrix $\hat{\mathcal{P}}_{\epsilon|V_{n,N}}^{\sharp}$ may be analysed along the same lines as $\mathcal{P}_{\epsilon|V_n}$ in the previous appendix. Its spectrum is contained for any $\epsilon > 0$ and any $r > 0$ in the convex hull of $A_{n,N}(r\mathbb{T}^1)$, which converges to the convex hull of $a_n(r\mathbb{T}^1)$ when $N \rightarrow \infty$.

References

- [1] Agam O and Blum G 2000 The leading Ruelle resonances of chaotic maps *Phys. Rev. E* **62** 1977–82
- [2] Andreev A V, Agam O, Altshuler B L and Simons B D 1996 Semiclassical field theory approach to quantum chaos *Nucl. Phys. B* **482** 536–66
- [3] Arnold V I and Avez A 1968 *Ergodic Problems of Classical Mechanics* (New York: Benjamin)
- [4] Baladi V 2001 Spectrum and statistical properties of chaotic dynamics *Prog. Math.* **201** 203–23
- [5] Baladi V and Baillif M 2002 Kneading determinants and spectra of transfer operators in higher dimensions, the isotropic case *Preprint math.DS/0211343/*
- [6] Baladi V and Young L-S 1993 On the spectra of randomly perturbed expanding maps *Commun. Math. Phys.* **156** 355–85
Baladi V and Young L-S 1994 *Commun. Math. Phys.* **166** 219–20 (erratum)
- [7] Bianucci P, Paz J P and Saraceno M 2002 Decoherence for classically chaotic quantum maps *Phys. Rev. E* **65** 046226
- [8] Blank M, Keller G and Liverani C 2002 Ruelle–Perron–Frobenius spectrum for Anosov maps *Nonlinearity* **15** 1905–73
- [9] Bogomolny E B 1992 Semiclassical quantization of multidimensional systems *Nonlinearity* **5** 805–66
- [10] Bonifacio R, Schwendimann P and Haake F 1971 Quantum statistical theory of superradiance *Phys. Rev. A* **4** 302–13 and 854–64
- [11] Böttcher A and Silbermann B 1999 *Introduction to Large Truncated Toeplitz Matrices* (Berlin: Springer)
- [12] Bouzouina A and De Bièvre S 1996 Equipartition of the eigenfunctions of quantized ergodic maps on the torus *Commun. Math. Phys.* **178** 83–105
- [13] Braun D 1999 Spectral properties of dissipative chaotic quantum maps *Chaos* **9** 730–7
Braun D 2001 *Dissipative Quantum Chaos and Decoherence (Springer Tracts in Modern Physics vol 172)* (Heidelberg: Springer)
- [14] Caldeira A O and Leggett A J 1985 Influence of damping on quantum interference: an exactly soluble model *Phys. Rev. A* **31** 1059–66
- [15] Childs A M, Chuang I L and Leung D W 2001 Realization of quantum process tomography in NMR *Phys. Rev. A* **64** 012314
Vandersypen L M K *et al* 2001 Experimental realization of Shor’s quantum factoring algorithm using nuclear magnetic resonance *Nature* **414** 883–7
- [16] Conley C and Zehnder E 1983 The Birkhoff–Lewis fixed point theorem and a conjecture of V I Arnold *Invent. Math.* **73** 33–49
- [17] Chuang I L and Nielsen M A 2000 *Quantum Computation and Quantum Information* (Cambridge: Cambridge University Press)
- [18] Cornfeld I P, Fomin S V and Sinai Ya G 1982 *Ergodic Theory* (Berlin: Springer)

- [19] Degli Esposti M, Graffi S and Isola S 1995 Classical limit of the quantized hyperbolic toral automorphisms *Commun. Math. Phys.* **167** 471–507
- [20] Fannjiang A and Wołowski L 2003 Noise induced dissipation in Lebesgue-measure preserving maps on d -dimensional torus *Preprint*
- [21] Garcia Mata I, Saraceno M and Spina M E 2003 Classical decays in decoherent quantum maps *Preprint* nlin.CD/0301025
- [22] Habib S, Shizume K and Zurek W H 1998 Decoherence, chaos and the correspondence principle *Phys. Rev. Lett.* **80** 4361
- [23] Hannay J H and Berry M V 1980 Quantization of linear maps on a torus-Fresnel diffraction by a periodic grating *Physica D* **1** 267–90
Degli Esposti M 1993 Quantization of the orientation preserving automorphisms of the torus *Ann. Inst. H Poincaré* **58** 323–41
- [24] Katok A and Hasselblatt B 1995 *Introduction to the Modern Theory of Dynamical Systems* (Cambridge: Cambridge University Press)
- [25] Keating J, Mezzadri F and Robbins J 1999 Quantum boundary conditions for torus maps *Nonlinearity* **12** 579–91
- [26] Khodas M, Fishman S and Agam O 2000 Relaxation to the invariant density for kicked rotor *Phys. Rev.* **62** 4769–83
Fishman S and Rahav S 2002 Relaxation and noise in chaotic systems *Lecture Notes (Ladek Winter School)* nlin.CD/0204068
- [27] Kifer Yu 1988 *Random Perturbations of Dynamical Systems* (Basel: Birkhäuser)
- [28] Kurlberg P and Rudnick Z 2001 On quantum ergodicity for linear maps of the torus *Commun. Math. Phys.* **222** 201–27
- [29] Kurlberg P 2002 On the order of unimodular matrices modulo integers *Preprint* math.NT/0202053
- [30] Lindblad G 1976 On the generators of quantum dynamical semigroups *Commun. Math. Phys.* **48** 119–30
- [31] Manderfeld C, Weber J and Haake F 2001 Classical versus quantum time evolution of (quasi-) probability densities at limited phase-space resolution *J. Phys. A: Math. Gen.* **34** 9893–905
Weber J, Haake F, Braun P A, Manderfeld C and Šeba P 2001 Resonances of the Frobenius–Perron operator for a Hamiltonian map with a mixed phase space *J. Phys. A: Math. Gen.* **34** 7195–211
- [32] Marklof J and Rudnick Z 2000 Quantum unique ergodicity for parabolic maps *Geom. Funct. Anal.* **10** 1554–78
- [33] Nonnenmacher S and Zirnbauer M R 2002 Det–det correlations for quantum maps: dual pair and saddle-point analyses *J. Math. Phys.* **43** 2214–40
- [34] Ostruszka A and Życzkowski K 2001 Spectrum of the Frobenius–Perron operator for systems with stochastic perturbation *Phys. Lett. A* **289** 306–12
- [35] Palla G, Vattay G, Voros A, Søndergaard N and Dettmann C-P 2001 Noise corrections to stochastic trace formulas *Found. Phys.* **31** 641–57
- [36] Parry W and Pollicott M 1990 Zeta functions and the periodic orbit structure of hyperbolic dynamics *Astérisque* vol 187–8, Société mathématique de France, Paris
- [37] Percival I and Vivaldi F 1987 Arithmetical properties of strongly chaotic motions *Physica D* **25** 105–30
- [38] Prosen T 2002 Chaotic resonances in quantum many-body dynamics *Preprint*
- [39] Reed M and Simon B 1972 *Methods of Modern Mathematical Physics, I: Functional Analysis* (New York: Academic)
- [40] Ruelle D 1986 Locating resonances for axiom A dynamical systems *J. Stat. Phys.* **44** 281–92
Ruelle D 1987 One-dimensional Gibbs states and axiom-A diffeomorphisms *J. Diff. Geom.* **25** 117–37
- [41] Rugh H H 1992 The correlation spectrum for hyperbolic analytic maps *Nonlinearity* **5** 1237–63
Rugh H H 1996 Generalized Fredholm determinants and Selberg zeta functions for axiom A dynamical systems *Ergod. Theory Dyn. Syst.* **16** 805–19
- [42] Tabor M 1983 A semiclassical quantization of area-preserving maps *Physica D* **6** 195–210
- [43] Takahashi K 1989 Distribution in classical and quantum mechanics *Prog. Theor. Phys. Suppl.* **98** 109–56
- [44] Zelditch S 1997 Index and dynamics of quantized contact transformations *Ann. Inst. Fourier* **47** 305–65